NUMERICAL SIMULATION OF TURBULENT NATURAL CONVECTION IN A RECTANGULAR ENCLOSURE WITH LOCALISED HEATING AND COOLING

BY

FRIDAH MAKENA MUGAMBI

BED (SCIE)

I56/CE/34548/2016

A dissertation submitted for partial fulfilment for the Degree of Masters of Science in The School of Pure and Applied Sciences Department of Mathematics Kenyatta University

2021

DECLARATION

I declare that this project is my own work and does not include anything which is the outcome of work done in collaboration and it has never been presented for a degree in any other University or any other award.

FRIDAH MAKENA MUGAMBI

REG NO. I56/CE/34548/2016

KENYATTA UNIVERSITY

SIGNATURE..... DATE.....

I confirm that this project was prepared by the candidate under my supervision;

DR.AWUOR KENNEDY OTIENO

SCHOOL OF PURE AND APPLIED SCIENCES

KENYATTA UNIVERSITY

SIGNATURE..... DATE.....

DEDICATION

I would like to dedicate this project to my Mum Winfred Muthoni, my husband Peterson Mutwiri, my sons Christian Baraka and Jayden Amani and my daughter Precious Zawadi for their love support and encouragement.

ACKNOWLEDGEMENT

I am greatly indebted to Dr. Kennedy Awuor of Mathematics, Kenyatta University for the guidance, suggestions, commitment, encouragement and supervision of this work.

I also acknowledge Mathematics Department of Kenyatta University for providing the necessary guidance without which the completion of this work would not have been possible.

Heartfelt gratitude go to my mum Winfred for her encouragement, my husband Peterson Mutwiri, my sons Jayden and Christian and my daughter Precious who were besides me throught the process of developing this project. Their understanding, encouragement and endurance during the most critical stage of my life, merits due recognition.

Above all, to God be the glory, honour and power for His immeasurable love mercies and grace that enabled my dream to become a reality.

TABLE OF CONTENT

LIST OF TABLES

LIST OF FIGURES

NOMENCLATURE

Symbol	Quantity
μ	Dynamic viscosity
Ɛ	Dissipation
ρ	Density
g	Acceleration due to gravity
C_p	Specific heat capacity
F_i	Body forces
V_t	Kinetic turbulent viscosity
C_u	Empirical constant
δ_{ij}	kronecker delta function
$\sigma_\varepsilon \& \sigma_k$	Prandtl for turbulent kinetic energy
Re	Reynolds number $\left\{\frac{inertialresistance}{viscousresistance} = \frac{\rho v l}{\eta}\right\}$
Pr	Prandtl number $\left(\frac{v}{\alpha} = \frac{viscous\ diffusion\ rate}{thermal\ diffusion\ rate} = \frac{C_p \mu}{K}\right)$
RANS	Reynolds Averaged Navier-Stokes Equations
ADI	Alternative Directional Implicit
FDE	Finite Difference Equation
Ar	Aspect Ratio
e	specific internal energy
L	Length of the enclosure
Ra	Rayleigh number
$\sigma_{k,1}, \sigma_{\omega,1}, \beta_{i,1}$	$\kappa - \omega$ closure

$\sigma_{k,2}, \sigma_{\omega,2}, \beta_{i,2}$	$\kappa - \omega$ closure
α_1, β_∞^*	SST closure constants

Greek symbol

α	Thermal diffusivity, m^2/s
β	Thermal expansion coefficient, 1/k
∇T	Temperature difference among cold and hot walls, k.
ν	Kinematic viscosity
μ	Dynamic viscosity
ξ	Non-dimensional temperature difference
ψ	Stream function
τ	Shear stress
ρ	Density of the fluid
∇t	Time interval
δ	Central difference operator
θ_f	Non-dimensional temperature difference $= \frac{T-T_c}{T_H-T_C}$
∂	Differential operator
∇	Del operator $i\frac{\partial}{\partial x} + j\frac{\partial}{\partial y}$
k-	Turbulent kinetic energy
ω-	Specific dissipation

Subscript

b	Boundary value
c	Cold wall
h	Hot wall
i,j	$i^{th} and\ j^{th}$ Mesh points along the x and y direction respectively.

Superscript

n	Current time step
n+1	New time step value
−	Mean value
·	Fluctuating component.

Roman symbols

Pr -	Prandtl number
u_j-	Velocity component
x_j-	Function of position

Abbreviations

FOTRAN	Formula translator
FVN	Finite volume method
Ar	Aspect ratio
RANS	Reynolds-averaged Napier stokes equation
Ra	Raleigh number

ABSTRACT

This study involves simulation of turbulent natural convection in a rectangular enclosure with localised heating and cooling. Numerical simulation of turbulent natural convection has been studied in the past using the k-epsilon (k-ε), k-omega (k-ω) and k-ω-SST turbulence models. Further research showed that the k-ω SST model performed better in terms of convergence of time than the k-ε and k-ω models. The study of natural convections in an enclosure has several applications from natural space, warming of household rooms to sections of engineering and atomic installations. This study involves numerical simulation of natural convention flow in a rectangular enclosure full of air using the k-ω- SST model with an objective of establishing the best position of the heater and the cooler for better distribution of heat in the enclosure. The transfer of heat due to natural convection inside a rectangular closed cavity was modelled to include the effect of Rayleigh number greater than or equal to 10^9.

The non-linear terms in averaged momentum and energy equation respectively were modeled using k-ω-SST model to close the governing equations.

The cavity was maintained at 303K on a square hot section midway on the extreme lower boundary of one of the vertical walls and at 283K on a square (twice in length and width the lower one) cold section midway on the extreme upper boundary on the same wall. The remaining part of this wall and the other five walls were adiabatic. The vorticity-vector potential, energy and the two equations for k-ω-SST model with boundary conditions were solved using finite difference method and FLUENT.

CHAPTER ONE INTRODUCTION

1.1 Background information

Natural convection is a mechanism or type of heat transport in which the motion of the fluid is not generated by an external source but only by the difference in densities in the fluid occurring due to temperature gradients.

Turbulent flow exists everywhere in nature from the jet stream to the Oceanic currents. Turbulent flows tend to occur at higher characteristic linear dimension. If Re>3500, then the flow is turbulent. They are characterized by the regular and disorderly movement of the particles of the fluid.

Turbulent flows are highly irregular and random, have high diffusivity and are described by a strong 3-D vortex generation mechanism called vortex stretching.

The study of natural convections in an enclosure has several applications from natural space, warming of household rooms to sections of engineering and atomic installations such as material processing, cooling of electronic equipment building technology as well as in passive heat removal system of a liquid metal nuclear rights actor characterised by four main features, dimension, dissipation, three dimensionality and length scales.

1.2 Problem Statement

Most flows encountered in real life situation e.g. in engineering are turbulent in nature. Due to this fact scientists have researched much on simulation of turbulent natural convection fluid flow.

Research on natural convection in an enclosure has been studied by Awuor (2012), whereby he investigated the performance of the three numerical models namely k-ε, k-ω and k-ω-SST with the aim of ascertaining the better approximation to experimental data in the process of predicting heat

transfer profiles in an air filled cavity. It was deduced that k-ω-SST was the best among the three models and hence the need to carry out further research using k-ω-SST model.

In his research Awuor (2012), heated one of the vertical faces and cooled the opposite vertical face of a rectangular cavity and hence the need to research on the numerical simulation of turbulent natural convection on a rectangle cavity when heat is supplied on a square portion midway on the extreme lower boundary of one of the vertical walls and cooled on a square (twice in length and width the lower one) portion midway on the extreme upper boundary on the same wall of a rectangular cavity.

1.3 Objectives

1.3.1 General objectives.

To conduct numerical simulation of turbulent natural convection in a rectangular enclosure with localised heating and cooling.

1.3.2 Specific Objectives

1. To formulate mathematical model for simulating natural convection.
2. To determine the change in velocity profiles, temperature profiles, convergence time, stability and accuracy of the numerical method.
3. To determine the convergence time, stability and accuracy of the numerical method.

1.3.3 Significance of study and anticipated output.

It is anticipated that when just a fraction of the vertical wall are heated and an equal fraction on the opposite vertical wall is cooled, then the computing resource requirement would be saved.

This study will be applicable to various engineering, farming or manufacturing practices e.g. in material processing, cooling of electronic equipment's warming of house rooms among others.

The data from this will provide optimal suitable velocity and temperature fields for manufacturing processes, preservation, packaging and storage. It will also give an insight on the best position to place the cooler for better distribution of the heat in the enclosure.

1.4 Definition of terms

Fluid

This is a substance that is capable of flowing and cannot preserve its shape unless it is restricted into a particular vessel and it continuously deforms on applying any slight shear force.

Compressible and incompressible flow

Compressible flow is a flow that undergoes an observable change in density within trending pressure.

Incompressible flow refers to the flow of fluid where in which the fluid density is constant.

Real and ideal flow

Real flow occurs for a fluid that is viscous in nature and there is a certain amount of resistance to flow.

An ideal flow involves the flow of a fluid which do not have viscosity and are incompressible. There is no shear resistance encountered in the flow.

Laminar and turbulent flow

A lamina flow is a flow in which a fluid flowing over a horizontal surface with steady flow and moves in the form of layers of different velocities which do not mix with each other.

A turbulent flow is a flow in which the liquid moves with a greater velocity than critical velocity. In this case the particles of the liquid become disorderly or irregular.

Steady and unsteady flow

A steady flow is one which the properties such as velocity, pressure, temperature and density are independent of time. Unsteady flow is a flow in which the properties are functions of time.

Convection

This is a type of heat transfer in fluids and occurs as a result of difference in temperature in varying areas of the fluid. Precisely, convection is a continuous circulation of fluids.

Natural convection

This is a type of flow in which the fluid motion is not generated by external source. The fluid motion is caused by density differences which are created by the temperature difference existing in the fluid mass.

Forced convection

This is a special type of heat transfer whereby the fluids are forced to move in order for it to increase the heat transfer. The motion of the fluid may be caused by external mechanic means e.g. a pump or a fun.

FLUENT

Is a “Flow Modelling Software” owned and distributed by ANSYS, Inc. It is utilized to demonstrate fluid flow inside a characterized geometry utilizing the standards of computational fluid dynamics.

CHAPTER 2: LITERATURE REVIEW

Different studies have been carried out on natural convection in enclosures. For instance, Altac and Ugurlubilek (2016) investigated unsteady natural convection heat transfer in 2D and 3D rectangular enclosures using a numerical method. In the study, the rectangular enclosures are heated and cooled from opposing isothermal walls that are vertical to each other and the other side walls of the rectangular enclosure were assumed to be adiabatic and smooth. Further, the fluid used in the study is air and the flow considered is turbulent. Commercial software called FLUENT 6.326 was used in solving 2D and 3D continuity equation in the unsteady state, Reynolds-Average Navier-stokes (RANS), as well as the average energy equation. The standard k-ε, Re-Normalization Group k-ε, Realizable k-ε, Reynolds stress Model, standard k-ε, and the shear stress transport k-ω models were used. Precisely, the performance of turbulence models on heat transfer rates was investigated for 2D and square enclosures and for 3- dimension rectangular enclosures with the slenderness ratio of 1 and 10^9 respectively. The assessment of heat transfer rates is done by the surface average mean Nusselt numbers over the wall that is hot and empirical power-law correlations are deduced. It is noted that identical Nusselt number predictions for the case of 2D RANS models when there are large Rayleigh numbers. Further, it is concluded that accurate mean Nusselt numbers are yielded from 3D RANS models.

Goodarzi *et al*, (2014) have also investigated the effective and accurate numerical method for simulation of natural convection heat transfer. The study of a heated square enclosure is carried out and for this purpose a FORTRAN code on the basis of Lattice Boltzmann method was used. The discretization of the LBM equations is done using the finite different method. FLUENT was used for comparison purpose in the simulation of the problem. The different discretization scheme such as First order upwind, power law and QUICK while the finite volume solver used are

SIMPLE and SIMPLEC algorithm then they were linked to the velocity pressure terms. The results derived from the model were compared with the experimental data. It was noted that less CPU usage time is required for the use of finite volume methods in comparison with LBM. Furthermore, the authors espoused that there is a faster convergence and higher accuracy when using a combination of the first order upwind and SIMPLEC. The convergence of the FVM discretization and pressure velocity linking methods converged after a closely similar number of iterations.

Further research on natural convection in an enclosure has been studied by Awuor (2012). Awuor (2012) investigated the performance of three numerical models namely k-ε, k-ω and k-ω- SST with the aim of ascertaining the better approximation to experimental data in the process of predicting heat transfer profiles in an air-filled cavity. In the study, the author used vorticity vector formulation in solving the momentum equation. It was noted that k-ε was not an effective model in the case where the temperature gradient at the boundaries is high but is useful in the free stream flows. In addition, it was deduced that k-ω-SST model gives accurate predictions under adverse pressure gradient and accounts for the transport shear stress. In terms of the convergence time, Awuor (2012) found that k-ω-SST model is a more accurate model to be used in layer simulation at a high-temperature gradient in comparison to k-ε model and k-ω model. Awuor (2012) further obtained numerical data using k-ω- SST model and noted that the room is stratified into the cold upper region, a warm lower region and a hot region between the window and heat.

Zimmermann and Groll (2014) undertook a numerical study on turbulent natural convection that had large eddy simulation. In the study, the acceleration in natural convection is driven by the differences in local densities and the pressure gradient. The increase in temperature gradients is used in determining the temperature distribution in the heated walls. In the numerical model, Zimmermann and Groll (2014) considered the change in density to occur due to change in

temperature difference. The author made a comparison of the numerical result with the data from an experimental setup. It was noted that the temperature and the velocity showed an asymmetry as a result of the non-Boussinesq effects of the fluid. In the study, a recommendation for the study of an incompressible turbulent model simulation is made.

Kimunguyi (2016) undertook a computational investigation of natural turbulent convection flow using primitive variables in the solution of the time average equations governing the flow instead of making use of the vorticity-vector potential formulation. In this study, Kimunguyi (2016) carried out a non-dimensionalization of the governing equations, the non-dimensional equations were then discretized using FVM and PISO and SIMPLEC algorithms were employed in the improvement of convergence time and speed. The method as well reduced the computational effort and there is a faster removal of the absolute error in the solution of flow. The author has concluded that the obtained velocity profiles and temperature profile are vital for use in ventilation systems for instance in the process of modelling the flow of air in a room.

Safaei *et al*. (2016) did a study on turbulent natural convection and laminar mixed convection flow of air in a room. The result of the study was then compared with data of other scientists. In the study, the author solved the flow as a turbulent mixed convection flow by employing RNG k-ε, standard k-ε, and RSM. Finite volume method was used in the solution of the governing differential equations. Safaei *et al*. (2016) noted that the flow is stationary at the centre of room at high Richardson Numbers. In addition , it is deduced that an increase in Richardson Number leads to a reduction in the maximum of Nusselt and hence a smaller Richardson Number implies a more rate of transfer of heat.

Edward *et al*. (2013) undertook a numerical study of turbulent natural convection flow in a 3-dimensional enclosure that had heaters on opposite sides of two windows placed opposite

to each other on adjacent walls. The governing equations of Newtonian fluid and the non-uniform mesh. The authors noted that the room is divided into numerous regions with the regions close to the heaters having higher temperatures as compared to the regions near the windows.

Wu and Lei (2015) studied turbulent natural convection in 2D and 3D with and without radiation transfer in heater cavities. Various Reynolds Average Navier-Stokes (RANS) turbulence model and the Discrete Ordinates radiation model were used in the numerical investigation. Further, Wu and Lei (2015) used quantitative and qualitative data for demonstration of the effects of three-dimensionality, thermal buoyancy condition and radiation transfer in surfaces that are horizontal. They derived simulation data from the numerical investigation are compared with the experimental data. The authors noted that when the radiation transfer is not accounted for the thermal boundary condition has an impact on the numerical solution on the horizontal surfaces. Moreover, it is deduced that variation of numerical results obtained when using three k-ε model is small. In the study , it is concluded that the k-ω- SST model had the best overall performance while k-ω model had the worst performance.

Khanal and Lei (2015) carried out a numerical investigation of the buoyancy induced a turbulent air flow in an inclined passive wall solar chimney that was attached to a roomk-ε model was employed in modelling the air turbulence in the solar chimney system. The investigation is carried out over the Rayleigh number range of $1.36 \times 10^{13} \leq 1.36 \times 10^{16}$ and the angle of inclination is between 0 and 6. The result in the study by Khanal and Lei (2015) indicates that there is a decrease in the amount of turbulent kinetic energy and turbulent intensity in the solar chimney with the increase in the angle of inclination.

Sajjadi and Kefayati (2015) undertook a Lattice Boltzmann simulation of turbulent natural convection with large eddy simulation in tall enclosures that are filled with air (Pr=0.71). High Rayleigh numbers ranging from 10^7 and 10^9 and an aspect ratio changes between 0.5 and 2 are used in performing the calculations. The author concluded that the average Nusselt number increases with the augmentation of Rayleigh numbers leading to a declination in the heat transfer in varying aspects ratios.

Joseph *et.al* (2018) carried out a Numerical investigation of turbulent natural convection in 3-D enclosure using k-ω-SST model and SIMPLEC Method. The statistical average process of mass, momentum and energy governing equations introduces unknown turbulent correlation into the mean flow equations which represent the turbulent transport of momentum, heat and mass which were modelled using k-ω-SST model. They found that both experimental data and simulation using SIMPLEC return a non-dimensional temperature of 0.5 at the core of the cavity and almost zero towards the cold and the natural turbulent flow is responsible for temperature distribution. In the similar work above, the location of the heater received no attention and hence the need to study numerical simulation of turbulent natural convection in a rectangular enclosure with localised heating and cooling on one side of the wall.

CHAPTER 3: EQUATIONS GOVERNING NATURAL CONVECTIONS IN TURBULENT FLOW

Introduction

The general laws governing fluid dynamics are the law of conservation of mass, the law of conservation of momentum and the law of conservation of energy. Most common occurring flows are turbulent in nature .The velocity, pressure and temperature at any point in the fluid vary rapidly and randomly with time and space. However the conservation laws also do apply in turbulent flows. Equations governing natural convections in turbulent flow are represented by partial differential equations. These equations are then decomposed by expressing fluid properties as the sum of a mean value and a fluctuating value, ($A = \bar{A} + A'$).

3.1 Continuity equation

Consider a control volume measuring *dxxdyxdz*

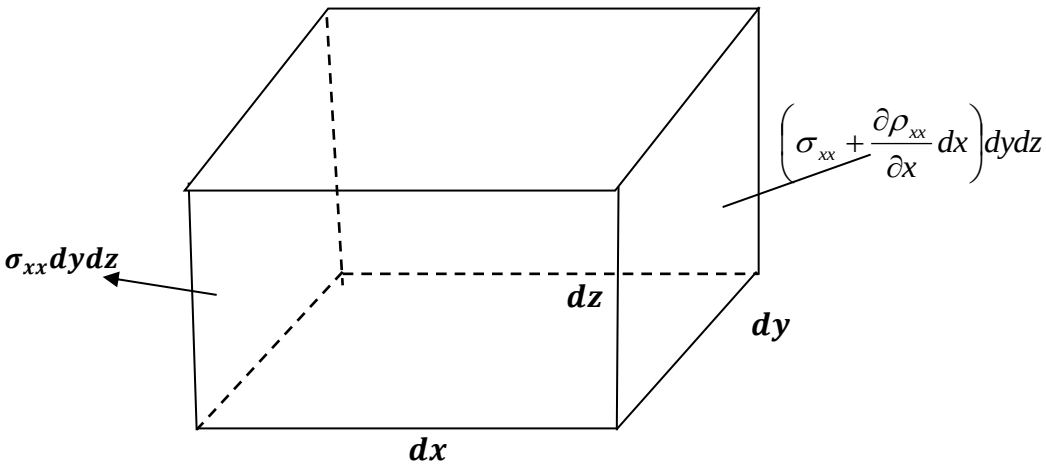

Figure 3.1: Control volume

Let mass density at P(x, y, z) be $\rho(x, y, z)$ Thus, average mass density throughout dv is,

Total mass $= m = \int_v \ \rho dv = \int_v \ \rho dx dy dz$ 3.1

Assuming inside dv there is no mass sinks or sources, then,

$\frac{dm}{dt}$ = rate upon which mass leaves or enters through surface ds

The mass flux through the surface is ρV, where V represents speed of the fluid. Thus, mass per unit time flowing through ds is

$\rho V . ds = \rho V .$ṅds 3.2

Where ṅ is the unit vector orthogonal to the surface.

Total flow rate of mass over the volume dv is

$\sum \rho V . ds = \oint \rho V . ds = \oint \rho V .$ ṅds 3.3

And it's equivalent to $-\frac{dm}{dt}, thus,$

$\frac{dm}{dt} = \frac{d}{dt} \oint \rho dv = -\oint \rho V .$ṅds 3.4

For fixed surface, derivative of total time within the volume integral can be taken as a partial derivative

$\int_v \ \frac{\partial p}{\partial t} dv = \oint_s \ \rho V .$ṅds 3.5

By Gauss theorem,

$\oint_s \ \rho V .$ ṅds = $\oint_v \ \nabla . (\rho V) dv$ 3.6

Thus substituting equation (3.6) to (3.5), we get

$$=\int_v \frac{\partial p}{\partial t}\, dv = -\int_v \nabla.(\rho V) dv$$

$$=\int_v [\frac{\partial p}{\partial t} + \nabla.(\rho V)] dv = 0 \qquad 3.7$$

Since it holds for any section and over any time interval, we conclude that the integrant in (3.7) must be identically be equal to zero, i.e.,

$$\frac{\partial \rho}{\partial t} + \nabla.(\rho V) = 0 \qquad 3.8$$

This is the general equation of mass conservation.

For incompressible flows ρ is constant and equation (3.7) reduces to

$$\rho \nabla \overline{V} + \overline{V} \nabla \rho = 0$$

$$\rho \nabla \overline{V} = 0$$

$$\nabla \overline{V} = 0 \qquad 3.9$$

For an incompressible flow, velocity field should be divergence free.

Since V is a velocity vector field, equation 3.8) can be written as;

$$\frac{\partial u}{\partial x} + \frac{\partial \mathrm{v}}{\partial y} + \frac{\partial w}{\partial z} = 0$$

3.2 Momentum conservation equation

The equation results from Newton's second law of motion

$F = Ma$

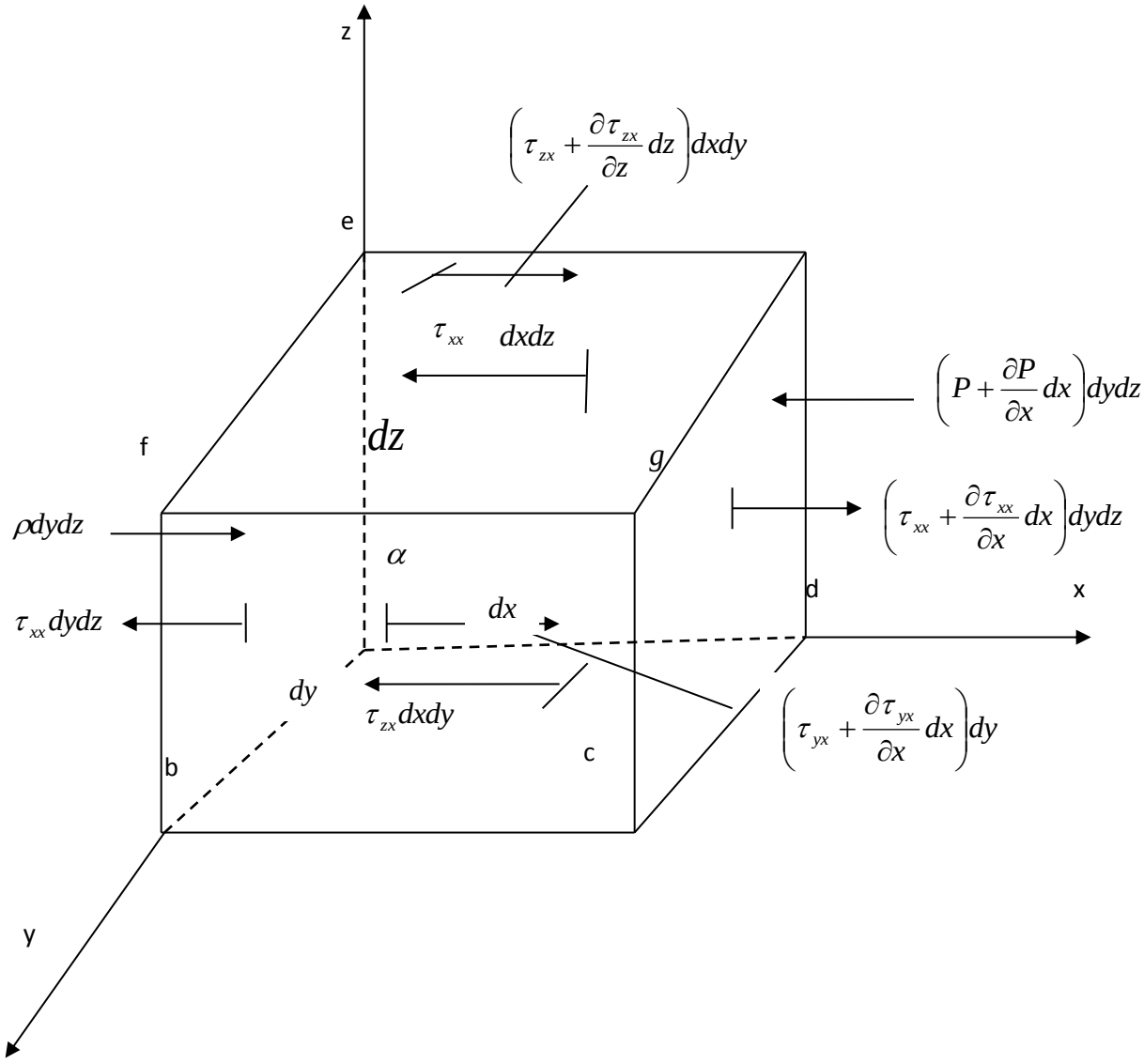

Figure 3.2 Small moving fluid components showing forces in x course

The net force on fluid component equivalents to product of its acceleration and mass according to Newton's second law on the moving fluid component.

That is, $\overline{F} = M\bar{a}$

Considering the x-component of the law,

$$F_x = Ma_x \qquad 3.10$$

where,

$a_x - x -$ component of acceleration

$F_x - x -$ component of force

Surface force (Fs) and body force (F_B) are the main forces acting on the component.

Considering fluid component weight as the only body force and letting g the body force per unit mass acting on the fluid component, with g as the x-component, the weight of fluid component in the x-direction will be given by

$$F_s = \rho g_x (dxdydz) \qquad 3.11$$

Where $dxdydz$ is the volume of fluid component.

The surface force due to stress exerted on the sides of the fluid elements are the shear stress, normal stress and pressure.

The figure above shows the surface forces in x-course.

On face $abed$, we have one shear force in negative x-course, $\tau_{zx}dxdy$ and on the opposite face, the face $efgh$ has a shear force of $\left(\tau_{zx}+\frac{\partial\tau_{zx}}{\partial z}dz\right)dxdy$ in the positive x-course. Similarly for face $adhe$, we have $\left(\tau_{yx}+\frac{\partial\tau_{yx}}{\partial y}dy\right)dxdz$ for the face $begf$.

For the face perpendicular to x-axis, that is, $abfe$, we have pressure force $Pdydz$ acting in positive x-direction and normal stress $\tau_{xx}dydz$ in negative x-direction while for the opposite face cdhg we have the pressure $\left(\tau_{xx}+\frac{\partial\tau_{xx}}{\partial x}dx\right)dydz$ which acts in the positive x-course.

Thus, the sum of surface forces in x-curse is

$$F_S=\left[\left(\tau_{xx}+\frac{\partial\tau_{xx}}{\partial x}dx\right)-\tau_{xx}\right]dydz+\left[\left(P+\frac{\partial P}{\partial x}dx\right)\right]dydz+\left[\left(\tau_{yx}+\frac{\partial\tau_{yx}}{\partial y}dy\right)-\tau_{yx}\right]dxdz$$

$$+\left[\left(\tau_{xx}+\frac{\partial\tau_{xx}}{\partial z}\right)-\tau_{zx}\right]dxdy$$

$$F_S=\left(-\frac{\partial P}{\partial x}+\frac{\partial\tau_{xx}}{\partial x}+\frac{\partial\tau_{yx}}{\partial y}+\frac{\partial\tau_{zx}}{\partial z}\right)dxdydz \qquad 3.12$$

Thus, total forces in x-course F_x is obtained by summing equations (3.11) and (3.12)

$$F_x=F_B+F_s$$

$$F_x = \left(-\frac{\partial P}{\partial x} + \frac{\partial \tau_{xx}}{\partial x} + \frac{\partial \tau_{yx}}{\partial y} + \frac{\partial \tau_{zx}}{\partial z}\right) dxdydz + \rho g_x \, dxdydz \quad 3.13$$

Considering the R.H.S. of equation 3.10, the mass of the component is constant and is given by:

$$m = \rho dxdydz \quad 3.14$$

The velocity components in the *z*, *y* and *x* directions of the fluid element is *w*, *v* and *u* respectively.

I.e. $w = \frac{dz}{dt}, v = \frac{dy}{dt}\ and\ u = \frac{dx}{dt}$

the rate of change of velocity is the acceleration of the fluid component thus, a_x is the rate of change of *u* which is the acceleration component in the x-direction, thus,

$$a_x = \frac{du}{dt}$$

Thus,

$$F_x = \rho \frac{du}{dt} dxdydz \quad 3.15$$

Combining eqns. (3.13) and (3.15) and dividing throughout by $dxdydz$, we get

$$\rho \frac{du}{dt} = -\frac{\partial P}{\partial x} + \frac{\partial \tau_{xx}}{\partial x} + \frac{\partial \tau_{yx}}{\partial y} + \frac{\partial \tau_{zx}}{\partial z} + \rho g_x, \quad 3.16a$$

Similarly, the *y* and *z* components become,

$$\rho \frac{dv}{dt} = -\frac{\partial P}{\partial y} + \frac{\partial \tau_{xy}}{\partial x} + \frac{\partial \tau_{yy}}{\partial y} + \frac{\partial \tau_{zy}}{\partial z} + \rho g_y \text{ and} \quad 3.16b$$

$$\rho \frac{dw}{dt} = -\frac{\partial P}{\partial x} + \frac{\partial \tau_{xz}}{\partial x} + \frac{\partial \tau_{yz}}{\partial y} + \frac{\partial \tau_{zz}}{\partial z} + \rho g_z \qquad 3.16c$$

Equations 3.16a, b and c are x, y and z component of equation of momentum. The equations are in non-conversation form since the fluid component is moving with the flow, and thus in honor of Englishman G. Stokes and Frenchman M. Navier, they are called the Navier-Stokes equations.

Conservation form

By writing

$$\rho \frac{du}{dt} = \rho \frac{\partial u}{\partial t} + \rho \vec{V} \cdot \nabla_u \qquad 3.17$$

Using the following derivative,

$$\frac{\partial(\rho u)}{\partial t} = \rho \frac{\partial u}{\partial t} + u \frac{\partial \rho}{\partial t}$$

$$\rho \frac{\partial u}{\partial t} = \frac{\partial(\rho u)}{\partial t} - u \frac{\partial \rho}{\partial t} \qquad 3.18$$

Using the divergence theorem,

$$\nabla.\left(\rho u \overline{V}\right) = u\nabla - \left(\rho \overline{V}\right) + \left(\rho \overline{V}\right).\nabla u$$

$$\rho \overline{V}.\nabla u = \nabla.\left(\rho u \overline{V}\right) - u\nabla.\left(\rho \overline{V}\right) \qquad 3.19$$

Replacing equations, 3.18 and 3.19 into e.g. 3.17, we get

$$\rho \frac{du}{dt} = \frac{\partial(\rho u)}{\partial t} - u \frac{\partial \rho}{\partial t} - u\nabla \cdot \left(\rho \vec{V}\right) + \nabla \cdot \left(\rho u \vec{V}\right)$$

$$\rho \frac{du}{dt} = \frac{\partial(\rho u)}{\partial t} - u\left[\frac{\partial \rho}{\partial t} - \nabla \cdot \left(\rho \vec{V}\right)\right] + \nabla \cdot \left(\rho u \vec{V}\right) \qquad 3.20$$

Since the continuity equation is zero, hence the term in brackets in equation .3.20 is zero thus equation 3.20 simplifies to;

$$\rho \frac{du}{dt} = \frac{\partial(\rho u)}{\partial t} + \nabla \cdot \left(\rho u \vec{V}\right) \quad 3.21$$

Replacing equation 3.21 into equation 3.16a, we get

$$\frac{\partial(\rho u)}{\partial t} + \nabla \cdot \left(\rho u \vec{V}\right) = -\frac{\partial P}{\partial x} + \frac{\partial \tau_{xx}}{\partial x} + \frac{\partial \tau_{yx}}{\partial y} + \frac{\partial \tau_{zx}}{\partial z} + \rho g_x \quad 3.22a$$

Similarly, for equations 3.16b and c we obtain,

$$\frac{\partial(\rho v)}{\partial t} + \nabla \cdot \left(\rho v \vec{V}\right) = -\frac{\partial P}{\partial y} + \frac{\partial \tau_{xy}}{\partial x} + \frac{\partial yy}{\partial y} + \frac{\partial \tau_{zy}}{\partial z} + \rho g_y \quad 3.22b$$

and

$$\frac{\partial(\rho w)}{\partial t} + \nabla \cdot \left(\rho w \vec{V}\right) = -\frac{\partial P}{\partial z} + \frac{\partial \tau_{xz}}{\partial x} + \frac{\partial yz}{\partial y} + \frac{\partial \tau_{zz}}{\partial z} + \rho g_z \quad 3.22c$$

The above equations are the conservation form of Navier-stokes equations.

3.3 The Energy Equation

It results from first law of thermodynamics that states that the change in interior energy of a system is equivalent to the heat into the system less the work done by the system.

Mathematically it is expressed as

$$\Delta U = Q - W$$

Where W is the work done by the system, Q is the beat added to the system and ΔU is the change in internal energy.

I.e.	*Rate of change of energy inside the fluid component*	=	*Net flux of heat into the component*	+	*Rate of work done on the component due to surface and body force*	3.23

We start by evaluating on moving fluid component, the rate of work done due to surface and body forces. It can be shown that the product of component of velocity in the direction of force and the force is equal to the rate of doing work by a force exerted on a body in motion. Therefore, on the fluid component moving with speed v, the rate of work done by the body force is given by $\rho \vec{f}.\vec{v}(dxdydz)$.

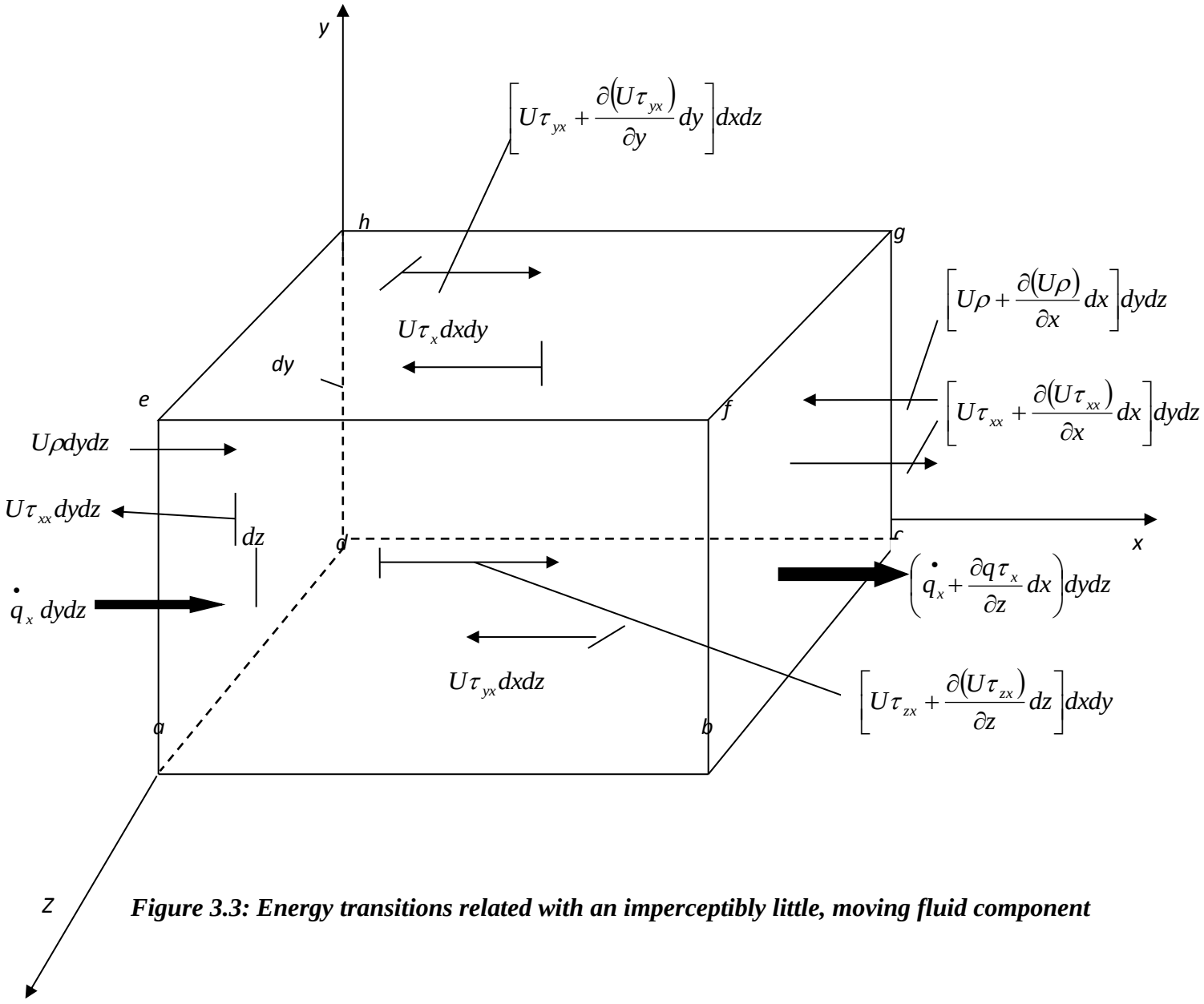

Figure 3.3: Energy transitions related with an imperceptibly little, moving fluid component

We consider surface forces (pressure in addition to shear and normal stresses), acting in x-course (Figure 3.3). On the moving fluid component, the rate of work done by surface force in x-segment of speed u, duplicated by forces, for example, on abed face, rate of doing work by $\tau_{yz}dxdz$ is $u\tau_{yz}dxdz$ with other faces having same expressions.

On fluid component, to acquire the total rate of doing word by surface force, it should be noted that negative work is done by forces in the negative x-course and positive work for positive x-courses.

Considering the pressure force on the face '$begf$' and '$adhe$' in Figure 3.2, total rate of doing work by shear and pressure stress in x-course is given by

$$\left[u\rho - \left(u\rho + \frac{\partial(u\rho)}{\partial x}\right)\right]dydz = -\frac{\partial(u\rho)}{\partial x}dxdydz,$$

and

$$\left[\left(u\tau_{yx} + \frac{\partial(u\tau_{yx})}{\partial y}\right) - u\tau_{yx}\right]dxdz = \frac{\partial(u\tau_{yx})}{\partial y}dxdydz$$

Bearing in mind all surface forces in figure 3.3, the net rate of doing work on the moving fluid component is;

$$\left[-\frac{\partial(u\rho)}{\partial x} + \frac{\partial(u\tau_{xx})}{\partial x} + \frac{\partial(u\tau_{yx})}{\partial x} + \frac{\partial(u\tau_{zx})}{\partial x}\right]dxdydz$$

The expression gives just surface force in x-course; comparable expressions can be acquired for x-and z-courses. Incorporating the body force input and considering all surface forces, net rate of doing work on mobbing fluid component becomes,

$$\begin{Bmatrix} Rate\ of\ work\ done \\ on\ the\ element\ due \\ to\ the\ boyd\ forces \end{Bmatrix} = \begin{bmatrix} \frac{\partial(u\rho)}{\partial x} + \frac{\partial(v\rho)}{\partial y} + \frac{\partial(w\rho)}{\partial z} + \\ \frac{\partial(u\tau_{xx})}{\partial x} + \frac{\partial(u\tau_{yx})}{\partial y} + \frac{\partial(u\tau_{zx})}{\partial z} + \\ \frac{\partial(v\tau_{xx})}{\partial x} + \frac{\partial(v\tau_{yy})}{\partial y} + \frac{\partial(v\tau_{zy})}{\partial z} + \\ \frac{\partial(w\tau_{xx})}{\partial x} + \frac{\partial(w\tau_{yy})}{\partial y} + \frac{\partial(w\tau_{zy})}{\partial z} \end{bmatrix} + dxdydz + \rho\vec{f} \cdot \vec{v} \quad 3.24$$

We now turn to the second term of equation (3.23), that is, net motion into the component. The volumetric warming causes heat transition, for example, ingestion or outflows of radiation, heat exchange over the surface because of temperature inclinations, that is, thermal conduction.

We characterize q as the rate of accumulation of volumetric heat for each unit mass. As prior defined the mass of fluid component in motion in $\rho dxdydz$, thus, we hen acquire.

$$\begin{Bmatrix} Volumetric\ heating\ of\ the \\ element \end{Bmatrix} = \rho q dxdydz \quad 3.25$$

In Figure 3.3, the heat exchanged into a moving fluid by thermal conduction component crosswise over face '$adhe$' is $q_x dxdydz$ where qx is heat moved in x-course per unit area per unit time by thermal conduction. The heat exchanged out of the component crosswise over face '$bcgf$' is,

$$\left[q_x + \left(\frac{\partial q_x}{\partial x}\right) dx\right] dydz,$$

Therefore, the net moved heat by thermal conduction in the x-course into the fluid component is;

$$\left[q_x - \left(q_x + \frac{\partial q_x}{\partial x}\right) dx\right] dydz = -\frac{\partial q_x}{\partial x} dxdydz$$

Considering heat exchanging the y-direction over other faces in figure 3.3, we acquire,

$$\begin{Bmatrix} Fluid\ component\ heating \\ by\ thermal\ conductivity \end{Bmatrix} = -\left(\frac{\partial \dot{q}_x}{\partial x} + \frac{\partial \dot{q}_y}{\partial y} + \frac{\partial \dot{q}_z}{\partial z}\right) dxdydz \qquad 3.26$$

Summing up equations (3.25) and (3.26), gives the net heat flux into the element;

$$\begin{Bmatrix} Fluid\ component\ heating \\ by\ thermal\ conductivity \end{Bmatrix} = -\rho\dot{q} - \left(\frac{\partial \dot{q}_x}{\partial x} + \frac{\partial \dot{q}_y}{\partial y} + \frac{\partial \dot{q}_z}{\partial z}\right) dxdydz \qquad 3.27$$

Local temperature corresponds to heat exchange by thermal conduction;

$$\dot{q}_x = -k\frac{\partial T}{\partial x}\ ; \qquad \dot{q}_y = -k\frac{\partial T}{\partial y}\ ; \qquad \dot{q}_z = -k\frac{\partial T}{\partial z};$$

Where k is the thermal conductivity.

Substituting these in equation (3.35) we have,

$$\begin{Bmatrix} Fluid\ component\ heating \\ by\ thermal\ conductivity \end{Bmatrix} = -\frac{\partial}{\partial x}\left(k\frac{\partial T}{\partial x}\right) + \frac{\partial}{\partial y}\left(k\frac{\partial T}{\partial y}\right) + \frac{\partial}{\partial z}\left(k\frac{\partial T}{\partial z}\right) dxdydz \qquad 3.28$$

At last, we consider time rate of change of energy inside fluid component. Moving fluid aggregate energy for each unit mass is the entirely of its kinetic energy for each unit mass, $V^2/2$ and inner energy per unit mass, e. Thus, aggregate energy is $e + V^2/2$. Since the fluid component is in motion the time-rate-of-change of energy for each unit mass in given by significant derivatives.

Taking fluid component mass as $\rho dxdydz$, we have;

$$\begin{Bmatrix} Rate\ of\ change\ of \\ energy\ inside \\ the\ fluid\ element \end{Bmatrix} = \rho \frac{D}{Dt}\left(e + \frac{V^2}{2}\right) dxdydz \qquad 3.29$$

The last type of the energy is gotten by substituting equations. (3.24), (3.28) and (3.29) into equation (3.23) obtaining;

$$\rho \frac{v}{vz} = \rho q + \frac{\partial}{\partial x}\left(k \frac{\partial T}{\partial x}\right) + \frac{\partial}{\partial y}\left(k \frac{\partial T}{\partial y}\right) + \frac{\partial}{\partial z}\left(k \frac{\partial T}{\partial z}\right) - \left(\frac{\partial [u\rho]}{\partial x} + \frac{\partial [v\rho]}{\partial y} + \frac{\partial [w\rho]}{\partial z}\right) + \frac{\partial (u\tau_{xx})}{\partial x} + \frac{\partial \lfloor u\tau_{yx} \rfloor}{\partial y} + \frac{\partial \lfloor u\tau_{zz} \rfloor}{\partial y} +$$

$$\frac{\partial \lfloor v\tau_{xy} \rfloor}{\partial x} + \frac{\partial \lfloor v\tau_{yy} \rfloor}{\partial y} + \frac{\partial \lfloor v\tau_{zy} \rfloor}{\partial y} + \frac{\partial \lfloor w\tau_{xz} \rfloor}{\partial x} + \frac{\partial \lfloor w\tau_{yz} \rfloor}{\partial y} + \frac{\partial \lfloor w\tau_{zz} \rfloor}{\partial y} + \rho \vec{f}\vec{v} \qquad 3.30$$

This is the energy equation in non-conservation form. It's worth to note that it's in form of the total energy, $e + \frac{v^2}{2}$. Normally, the equation is written such that it involves the internal energy *e* which is derived as

Rewriting equations 3.22 a, b and c as from Navier stoke, in non-conservative form, we have;

$$\left.\begin{aligned} \rho \frac{Du}{Dt} &= -\frac{\partial \rho}{\partial x} + \frac{\partial \tau_{xx}}{\partial x} + \frac{\partial \tau_{yx}}{\partial y} + \frac{\partial \tau_{zx}}{\partial z} + \rho f_x, \\ \rho \frac{Dv}{Dt} &= -\frac{\partial \rho}{\partial y} + \frac{\partial \tau_{xy}}{\partial x} + \frac{\partial \tau_{yy}}{\partial y} + \frac{\partial \tau_{zy}}{\partial z} + \rho f_y, \\ \rho \frac{Dw}{Dt} &= -\frac{\partial \rho}{\partial z} + \frac{\partial \tau_{xz}}{\partial x} + \frac{\partial \tau_{yz}}{\partial y} + \frac{\partial \tau_{zz}}{\partial z} + \rho f_z, \end{aligned}\right\} \qquad 3.31$$

Multiplying each of the equations, equation (3.31) by $u, v,$ and w respectively,

$$\rho \frac{D\left(\frac{u^2}{2}\right)}{D} = -u\frac{\partial p}{\partial x} + u\frac{\partial \tau_{xx}}{\partial x} + u\frac{\partial \tau_{yx}}{\partial y} + u\frac{\partial \tau_{zx}}{\partial z} + \rho u f_x \quad 3.32a$$

$$\rho \frac{D\left(\frac{v^2}{2}\right)}{D} = -v\frac{\partial p}{\partial x} + v\frac{\partial \tau_{xy}}{\partial x} + v\frac{\partial \tau_{yy}}{\partial y} + v\frac{\partial \tau_{zy}}{\partial z} + \rho v f_y \quad 3.32b$$

$$\rho \frac{D\left(\frac{w^2}{2}\right)}{D} = -w\frac{\partial p}{\partial y} + w\frac{\partial \tau_{xz}}{\partial x} + w\frac{\partial \tau_{yz}}{\partial y} + w\frac{\partial \tau_{zz}}{\partial z} + \rho w f_z \quad 3.32c$$

Adding equations (3.32 a, b and c) and noting that $u^2 + v^2 + w^2 = V^2$ we obtain;

$$\rho \frac{DV^2/2}{Dt} = -u\frac{\partial p}{\partial x} - v\frac{\partial p}{\partial x} - w\frac{\partial p}{\partial y} + u\left(\frac{\partial \tau_{xx}}{\partial x} + \frac{\partial \tau_{yx}}{\partial y} + \frac{\partial \tau_{zx}}{\partial z}\right) + v\left(\frac{\partial \tau_{xy}}{\partial x} + \frac{\partial \tau_{yy}}{\partial y} + \frac{\partial \tau_{zy}}{\partial z}\right) + w\left(\frac{\partial \tau_{xz}}{\partial x} + \frac{\partial \tau_{yz}}{\partial y} + \frac{\partial \tau_{zz}}{\partial z}\right) + \rho\left(uf_x + vf_y + wf_z\right) \quad 3.33$$

Subtracting equation (3.33) from equation (3.30), noting that $\rho\vec{f}\cdot\vec{v} = \rho\left(uf_x + vf_y + wf_z\right)$

We have;

$$\rho\frac{De}{Dt} = \rho q + \frac{\partial}{\partial x}\left(k\frac{\partial T}{\partial x}\right) + \frac{\partial}{\partial y}\left(k\frac{\partial T}{\partial y}\right) + \frac{\partial}{\partial z}\left(k\frac{\partial T}{\partial z}\right) - \rho\left(\frac{\partial u}{\partial x} + \frac{\partial v}{\partial y} + \frac{\partial w}{\partial z}\right) + \tau_{xx}\frac{\partial u}{\partial x} + \tau_{yx}\frac{\partial u}{\partial y} + \tau_{zx}\frac{\partial u}{\partial z} + \tau_{xy}\frac{\partial v}{\partial x} + \tau_{yy}\frac{\partial v}{\partial y} + \tau_{zy}\frac{\partial v}{\partial z} + \tau_{xz}\frac{\partial w}{\partial x} + \tau_{yz}\frac{\partial w}{\partial y} + \tau_{zz}\frac{\partial w}{\partial z} \quad 3.34$$

In terms of internal energy, equation (3.34) is the energy equation. Note that it does not explicitly contain the body force when it is written in terms of e, since the terms have cancelled. Still equation (3.34) is in non- conservation form. We note that,

$\tau_{xy} = \tau_{yx} = \tau_{xz} = \tau_{zx} = \tau_{yz} = \tau_{zy}$.

Thus rewriting equation (3.34) we get,

$$\rho \frac{De}{Dt} = \rho q + \frac{\partial}{\partial x}\left(k \frac{\partial T}{\partial x}\right) + \frac{\partial}{\partial y}\left(k \frac{\partial T}{\partial y}\right) + \frac{\partial}{\partial z}\left(k \frac{\partial T}{\partial z}\right) - \rho\left(\frac{\partial u}{\partial x} + \frac{\partial v}{\partial y} + \frac{\partial w}{\partial z}\right) + \tau_{xx}\frac{\partial u}{\partial x} + \tau_{yy}\frac{\partial v}{\partial y} + \tau_{zz}\frac{\partial w}{\partial z} +$$

$$\tau_{yx}\left(\frac{\partial u}{\partial y} + \frac{\partial v}{\partial x}\right) + \tau_{zx}\left(\frac{\partial u}{\partial z} + \frac{\partial w}{\partial x}\right) + \tau_{zy}\left(\frac{\partial v}{\partial z} + \frac{\partial w}{\partial y}\right) \quad 3.35$$

Using the definitions of normal the viscous stress and shear stress given (3.35) becomes,

$$\rho \frac{De}{Dt} = \rho q + \frac{\partial}{\partial x}\left(k \frac{\partial T}{\partial x}\right) + \frac{\partial}{\partial y}\left(k \frac{\partial T}{\partial y}\right) + \frac{\partial}{\partial z}\left(k \frac{\partial T}{\partial z}\right) - \rho\left(\frac{\partial u}{\partial x} + \frac{\partial v}{\partial y} + \frac{\partial w}{\partial z}\right) + \lambda\left(\frac{\partial u}{\partial x} + \frac{\partial v}{\partial y} + \frac{\partial w}{\partial z}\right)^2 +$$

$$\mu\left[2\left(\frac{\partial u}{\partial x}\right)^2 + 2\left(\frac{\partial v}{\partial y}\right)^2 + 2\left(\frac{\partial w}{\partial z}\right)^2 + \left(\frac{\partial u}{\partial y} + \frac{\partial v}{\partial x}\right)^2 + \left(\frac{\partial u}{\partial z} + \frac{\partial w}{\partial x}\right)^2 + \left(\frac{\partial v}{\partial z} + \frac{\partial w}{\partial y}\right)^2\right] \quad 3.36$$

Equation (3.36) is a form of energy equation completely in terms of flow-field variables. Same replacement can be made into equation (3.30). In conservation form, the energy equation can be found as follows;

Considering the LHS of the equation (3.36) and from substantial derivative definition;

$$\rho \frac{De}{Dt} = \rho \frac{\partial e}{\partial t} + \rho V.Ve \quad 3.37$$

$$\frac{\partial(\partial e)}{\partial t} = \rho \frac{\partial e}{\partial t} + e\frac{\partial \rho}{\partial t} \;\; or \;\; \rho \frac{\partial e}{\partial t} = \frac{\partial(\rho e)}{\partial t} - e\frac{\partial \rho}{\partial t} \quad 3.38$$

From the vector identity regarding divergence of the product of a vector and a scalar,

$$\nabla.\left(\rho e\vec{V}\right) = e\vec{V}.\left(\rho\vec{V}\right) + \rho\vec{V}.e\vec{V} \quad 3.39$$

Substitute equations (3.38) and (3.39) into equation (3.37) we have;

$$\rho\frac{De}{Dt} = \frac{\partial(\rho e)}{\partial t} - e\left[\frac{\partial\rho}{\partial t} + \nabla.\left(\rho\vec{V}\right)\right] + \nabla.\left(\rho e\vec{V}\right) \quad 3.40$$

The expression in square brackets in equation (3.40) is zero

Thus, equation (3.40) becomes

$$\rho\frac{De}{Dt} = \frac{\partial(\rho e)}{\partial t} + \nabla.\left(\rho e\vec{V}\right) \quad 3.41$$

Replacing equation (3.41) into equation (3.36), we get

$$\frac{\partial(\rho e)}{\partial t} + \nabla.\rho = \rho q + \frac{\partial}{\partial x}\left(k\frac{\partial T}{\partial x}\right) + \frac{\partial}{\partial y}\left(k\frac{\partial T}{\partial y}\right) + \frac{\partial}{\partial z}\left(k\frac{\partial T}{\partial z}\right) - p\left(\frac{\partial u}{\partial x} + \frac{\partial v}{\partial y} + \frac{\partial w}{\partial z}\right) + \lambda\left(\frac{\partial u}{\partial x} + \frac{\partial v}{\partial y} + \frac{\partial w}{\partial z}\right)^2 +$$

$$\mu\left[2\left(\frac{\partial u}{\partial x}\right)^2 + 2\left(\frac{\partial v}{\partial y}\right)^2 + 2\left(\frac{\partial w}{\partial z}\right)^2 + \left(\frac{\partial u}{\partial y} + \frac{\partial v}{\partial x}\right)^2 + \left(\frac{\partial u}{\partial z} + \frac{\partial w}{\partial x}\right)^2 + \left(\frac{\partial v}{\partial z} + \frac{\partial w}{\partial y}\right)^2\right] \quad 3.42$$

Equation (3.24) is written in terms of the internal energy and is the energy equation in conservation form.

Similarly, in form of total energy, the conservation form of energy equation, can be written as;

$$\frac{\partial}{\partial t}\left[\rho\left(e + \frac{v^2}{2}\right)\right] + \nabla.\left[\rho\left(e + \frac{v^2}{2}\vec{v}\right)\right] = \rho q + \frac{\partial}{\partial x}\left(k\frac{\partial T}{\partial x}\right) + \frac{\partial}{\partial y}\left(k\frac{\partial T}{\partial y}\right) + \frac{\partial}{\partial z}\left(k\frac{\partial T}{\partial z}\right) - \frac{\partial(u\rho)}{\partial x} - \frac{\partial(v\rho)}{\partial y} -$$

$$\frac{\partial(w\rho)}{\partial z} + \frac{\partial(u\tau_{xx})}{\partial x} + \frac{\partial(u\tau_{yx})}{\partial y} + \frac{\partial(u\tau_{zx})}{\partial z} + \frac{\partial(u\tau_{xy})}{\partial x} + \frac{\partial(u\tau_{yy})}{\partial y} + \frac{\partial(u\tau_{zy})}{\partial z} + \frac{\partial(u\tau_{zx})}{\partial x} + \frac{\partial(u\tau_{zy})}{\partial y} + \frac{\partial(u\tau_{zz})}{\partial z} + \rho\vec{f}.\vec{v}.$$

In Cartesian coordinate system, the governing equations for incompressible fluid flow become;

Mass conservation (continuity equation) equation

$$\frac{\partial u}{\partial x}+\frac{\partial v}{\partial y}+\frac{\partial w}{\partial z}=0$$

Momentum (Navier stokes) equations

x-direction:

$$\rho\left(\frac{\partial u}{\partial t}+u\frac{\partial u}{\partial x}+v\frac{\partial u}{\partial y}+w\frac{\partial u}{\partial z}\right)=F_x-\frac{\partial p}{\partial x}+\mu\left(\frac{\partial^2 u}{\partial x^2}+\frac{\partial^2 u}{\partial y^2}+\frac{\partial^2 u}{\partial z^2}\right)$$

y-direction:

$$\rho\left(\frac{\partial v}{\partial t}+u\frac{\partial v}{\partial x}+v\frac{\partial v}{\partial y}+w\frac{\partial v}{\partial z}\right)=F_y-\frac{\partial p}{\partial y}+\mu\left(\frac{\partial^2 v}{\partial x^2}+\frac{\partial^2 v}{\partial y^2}+\frac{\partial^2 v}{\partial z^2}\right)$$

z-direction:

$$\rho\left(\frac{\partial w}{\partial t}+u\frac{\partial w}{\partial x}+v\frac{\partial w}{\partial y}+w\frac{\partial w}{\partial z}\right)=F_z-\frac{\partial p}{\partial z}+\mu\left(\frac{\partial^2 w}{\partial x^2}+\frac{\partial^2 w}{\partial y^2}+\frac{\partial^2 w}{\partial z^2}\right)$$

Energy equation

$$\rho C_p\left(\frac{\partial T}{\partial t}+u\frac{\partial T}{\partial x}+v\frac{\partial T}{\partial y}+w\frac{\partial T}{\partial z}\right)=k\left(\frac{\partial^2 T}{\partial x^2}+\frac{\partial^2 T}{\partial y^2}+\frac{\partial^2 T}{\partial z^2}\right)+\Phi$$

where

$$\Phi=\mu\left\{2\left[\left(\frac{\partial u}{\partial x}\right)^2+\left(\frac{\partial v}{\partial y}\right)^2+\left(\frac{\partial w}{\partial z}\right)^2\right]+\left(\frac{\partial u}{\partial y}+\frac{\partial v}{\partial x}\right)^2+\left(\frac{\partial u}{\partial z}+\frac{\partial w}{\partial x}\right)^2+\left(\frac{\partial v}{\partial z}+\frac{\partial w}{\partial y}\right)^2\right\}$$

3.4 Reynolds Decomposition

The statistical averaging is necessary to estimate random fluctuations for time dependent nature of turbulence with extensive variety of scales.

This is a mathematical method that separates averaged and fluctuating part of the quantity, for instance, $u = \bar{u} + u'$ where $\bar{u}$ denotes time averaged of u known as steady part and u' as the perturbations or fluctuating part. It lets us simplify the Navier Stokes Equations by replacing the sum of the fluctuating and steady part to the velocity profile and taking the average value. The equation that results comprises a non-linear called Reynolds stress which gives turbulence.

Statistical averaging of differential equations

The earliest attempts at developing Mathematical description the closure problem was performed by Boussinesq (1877) with introduction of concept of the eddy viscosity. The origin of time averaging Navier Stokes equation dates back to the late 19th century when Reynolds (1895) published results from his research on turbulence.

The differential equations of energy, momentum and mass balances express fundamental physical laws and therefore hold for turbulent flow. If all the perturbations acting on the flow can be mathematically modelled, then these equations can be solved for the flow properties e.g. pressure and velocity. An easier task is to solve time averaged versions of these equations in which some of the fluctuation contributions are averaged out.

$$u = \bar{u} + u' \qquad 3.4.1a$$

$$v = \bar{v} + v' \qquad 3.4.1b$$

$$p = \bar{p} + p' \qquad 3.4.1c$$

$$\rho = \bar{\rho} + \rho' \qquad 3.4.1d$$

$$T = \bar{T} + T' \qquad 3.4.1e$$

and time averaged rules

$$\frac{1}{T}\int_0^T u dt = \bar{u} \quad and \qquad \frac{1}{T}\int_0^T u' dt = \overline{u'} = 0$$

$$\frac{1}{T}\int_0^T v dt = v \quad and \qquad \frac{1}{T}\int_0^T v' dt = \overline{v'} = 0$$

$$\frac{1}{T}\int_0^T p dt = \bar{p} \quad and \qquad \frac{1}{T}\int_0^T p' dt = \overline{p'} = 0$$

$$\frac{1}{T}\int_0^T \rho dt = \bar{\rho} \quad and \qquad \frac{1}{T}\int_0^T \rho' dt = \overline{\rho'} = 0$$

With t being a large interval of time.

The following rules as well apply during time averaging;

$$\bar{f} = \bar{f}, \qquad \overline{f+g} = \bar{f} + \bar{g}, \qquad \bar{f}.\bar{g} = \bar{f}.\bar{g},$$

$$\overline{\frac{\partial f}{\partial x}} = \frac{\partial f}{\partial x} \qquad \overline{\int f ds} = \int \bar{f} ds, \qquad \overline{f.g} \# \bar{f}.\bar{g}$$

Time averaged equation of continuity

Substituting 3.4.1c and 3.4.1d in 3.8 and time average, we obtain

$$\overline{\frac{\partial(\bar{\rho}+\rho')}{\partial t} + \nabla.(\bar{\rho}+\rho')(\bar{v}+v')} = 0 \qquad 3.4.2$$

This gives

$$\frac{\partial(\bar{\rho}+\overline{\rho'})}{\partial t} + \nabla.(\overline{\bar{\rho}\bar{v}} + \overline{\bar{\rho}v'} + \overline{\rho'\bar{v}} + \overline{\rho'v'}) = 0 \qquad 3.4.3$$

But $\overline{\bar{\rho}v'}$ and $\overline{\rho'\bar{v}}$ are equal to zero and $\overline{\bar{\rho}\bar{v}} = \bar{\rho}\bar{v}$

So equation 3.4.3 becomes

$\nabla.\bar{v} = 0$ (for incompressible fluid) 3.4.4

In Cartesian plane coordinate system, 3.4.4 becomes

$$\frac{\partial\bar{u}}{\partial x} + \frac{\partial\bar{v}}{\partial y} + \frac{\partial\bar{w}}{\partial z} = 0 \quad 3.4.5$$

Time averaged momentum equation

For a Newtonian, incompressible and with a constant viscosity fluid, Navier stokes equation 3.22 a and b we have;

$$\rho\left(\frac{\partial v}{\partial t} + v.\nabla v\right) = F_i - \nabla p + \mu\Delta v \quad 3.4.5$$

Substituting equations 3.4.1b and 3.4.1c in 3.4.5 and time averaging, we get

$$\overline{\rho\left[\frac{\partial(\bar{v}+v')}{\partial t} + (\bar{v}+v').\nabla(\bar{v}+v')\right]} = F_i - \overline{\nabla.(\bar{\rho}+p')} + \overline{\mu\Delta(\bar{v}+v')}$$

On working out, we get

$$\rho\left[\frac{\partial\overline{(\bar{v}+v')}}{\partial t} + \overline{\bar{v}.\nabla\bar{v}} + \overline{\bar{v}.\nabla v'} + \overline{v'\nabla\bar{v}} + \overline{v'\nabla v'}\right] = F_i - \overline{\nabla\bar{p}} + \mu\Delta\bar{\bar{v}} + \mu\Delta\overline{v'}$$

Which gives

$$\rho\left[\frac{\partial\bar{v}}{\partial t} + \bar{v}.\nabla\bar{v} + \overline{v'\nabla v'}\right] = F_i - \overline{\nabla\bar{p}} + \mu\Delta\overline{v'} \quad 3.4.6$$

Where $\overline{\bar{v}.\nabla v'}, \overline{v'\nabla\bar{v}}, \overline{v'}, \overline{p'}, \overline{v'} = 0$

And

$\nabla.\bar{v} = 0$

$$\rho\left[\frac{\partial\bar{v}}{\partial t}+\bar{v}.\nabla\bar{v}+\overline{\nabla.v'v'}\right]=F_i-\overline{\nabla\bar{p}}+\mu\Delta\bar{v}$$

Which gives;

$$\rho\left[\frac{\partial\bar{v}}{\partial t}+\bar{v}.\nabla\bar{v}+\right]=F_i-\overline{\nabla\bar{p}}+\mu\Delta\bar{v}-\overline{\nabla.\rho v'v'} \qquad 3.4.7$$

$\overline{\nabla.\rho v'v'}$ is called Reynold stress 3.4.8

In Cartesian place coordinate system, the time averaged NS equations for all direction becomes;

x-direction ;

$$\rho\left(\frac{\partial\bar{u}}{\partial t}+\bar{u}\frac{\partial\bar{u}}{\partial x}+\bar{v}\frac{\partial\bar{u}}{\partial y}+\bar{w}\frac{\partial\bar{u}}{\partial z}\right)$$

$$=F_x-\frac{\partial\bar{\rho}}{\partial x}+\mu\left(\frac{\partial^2\bar{u}}{\partial x^2}+\frac{\partial^2\bar{u}}{\partial y^2}+\frac{\partial^2\bar{u}}{\partial z^2}\right)-\rho\left(\frac{\partial\overline{u'u'}}{\partial x}+\frac{\partial\overline{u'v'}}{\partial y}+\frac{\partial\overline{u'w'}}{\partial z}\right)$$

y-direction;

$$\rho\left(\frac{\partial\bar{v}}{\partial t}+\bar{u}\frac{\partial\bar{v}}{\partial x}+\bar{v}\frac{\partial\bar{v}}{\partial y}+\bar{w}\frac{\partial\bar{v}}{\partial z}\right)$$

$$=F_Y-\frac{\partial\bar{\rho}}{\partial y}+\mu\left(\frac{\partial^2\bar{v}}{\partial x^2}+\frac{\partial^2\bar{v}}{\partial y^2}+\frac{\partial^2\bar{v}}{\partial z^2}\right)-\rho\left(\frac{\partial\overline{u'v'}}{\partial x}+\frac{\partial\overline{v'v'}}{\partial y}+\frac{\partial\overline{v'w'}}{\partial z}\right)$$

z-direction;

$$\rho\left(\frac{\partial\overline{w}}{\partial t}+\bar{u}\frac{\partial\overline{w}}{\partial x}+\bar{v}\frac{\partial\overline{w}}{\partial y}+\overline{w}\frac{\partial\overline{w}}{\partial z}\right)$$

$$=F_z-\frac{\partial\bar{\rho}}{\partial z}+\mu\left(\frac{\partial^2\overline{w}}{\partial x^2}+\frac{\partial^2\overline{w}}{\partial y^2}+\frac{\partial^2\overline{w}}{\partial z^2}\right)-\rho\left(\frac{\partial\overline{u'w'}}{\partial x}+\frac{\partial\overline{v'w'}}{\partial y}+\frac{\partial\overline{v'w'}}{\partial z}\right)$$

$$\rho\left(\frac{\partial\bar{u}}{\partial t}+\bar{u}\frac{\partial\bar{u}}{\partial x}+\bar{v}\frac{\partial\bar{u}}{\partial y}+\overline{w}\frac{\partial\bar{u}}{\partial z}\right)$$

$$=F_x-\frac{\partial\bar{\rho}}{\partial x}+\mu\left(\frac{\partial^2\bar{u}}{\partial x^2}+\frac{\partial^2\bar{u}}{\partial y^2}+\frac{\partial^2\bar{u}}{\partial z^2}\right)-\rho\left(\frac{\partial\overline{u'u'}}{\partial x}+\frac{\partial\overline{u'v'}}{\partial x}+\frac{\partial\overline{u'w'}}{\partial x}\right)$$

Time averaged energy equation

Substituting 3.4.1a,3.4.1b,3.4.1c and 3.4.1e in

$$\rho C_p\left(\frac{\partial T}{\partial t}+u\frac{\partial T}{\partial x}+v\frac{\partial T}{\partial y}+w\frac{\partial T}{\partial z}\right)=k\left(\frac{\partial^2T}{\partial x^2}+\frac{\partial^2T}{\partial y^2}+\frac{\partial^2T}{\partial z^2}\right)+\Phi$$

We obtain

$$\rho C_p\left(\frac{\partial(\bar{T}+T')}{\partial t}+(\bar{u}+u')\frac{\partial(\bar{T}+T')}{\partial t}+(\bar{v}+v')\frac{\partial(\bar{T}+T')}{\partial t}+(\overline{w}+w')\frac{\partial(\bar{T}+T')}{\partial t}\right)=k\left(\frac{\partial^2(\bar{T}+T')}{\partial x^2}+\right.$$

$$\left.\frac{\partial^2(\bar{T}+T')}{\partial y^2}+\frac{\partial^2(\bar{T}+T')}{\partial z^2}\right)+(\overline{\Phi}+\Phi') \qquad 3.4.9$$

Time averaging 3.4.9

$$\overline{\rho C_p\left(\frac{\partial(\bar{T}+T')}{\partial t}+(\bar{u}+u')\frac{\partial(\bar{T}+T')}{\partial t}+(\bar{v}+v')\frac{\partial(\bar{T}+T')}{\partial t}+(\bar{w}+w')\frac{\partial(\bar{T}+T')}{\partial t}\right)}=$$

$$\overline{k\left(\frac{\partial^2(\bar{T}+T')}{\partial x^2}+\frac{\partial^2(\bar{T}+T')}{\partial y^2}+\frac{\partial^2(\bar{T}+T')}{\partial z^2}\right)+\left(\overline{\bar{\Phi}+\Phi'}\right)} \quad 3.4.10$$

This yields

$$\rho C_p\left(\frac{\partial(\overline{\bar{T}+T'})}{\partial t}+(\overline{\bar{u}+u'})\frac{\partial(\overline{\bar{T}+T'})}{\partial t}+(\overline{\bar{v}+v'})\frac{\partial(\overline{\bar{T}+T'})}{\partial t}+(\overline{\bar{w}+w'})\frac{\partial(\overline{\bar{T}+T'})}{\partial t}\right)=k\left(\frac{\partial^2(\overline{\bar{T}+T'})}{\partial x^2}+\right.$$

$$\left.\frac{\partial^2(\overline{\bar{T}+T'})}{\partial y^2}+\frac{\partial^2(\overline{\bar{T}+T'})}{\partial z^2}\right)+\left(\overline{\bar{\Phi}+\Phi'}\right) \quad 3.4.11$$

Using the time averaged rules we get the following;

$$\rho C_p\left(\frac{\partial\bar{T}}{\partial t}+\bar{u}\frac{\partial\bar{T}}{\partial x}+\bar{v}\frac{\partial\bar{T}}{\partial y}+\bar{w}\frac{\partial\bar{T}}{\partial z}\right)=k\left(\frac{\partial^2\bar{T}}{\partial x^2}+\frac{\partial^2\bar{T}}{\partial y^2}+\frac{\partial^2\bar{T}}{\partial z^2}\right)-\frac{\partial C_p\overline{T'u'}}{\partial x_i}+\bar{\Phi} \quad 3.4.12$$

$\frac{\partial C_p\overline{T'u'}}{\partial x_i}$ represent the turbulent heat fluxes i.e perturbations of velocity and temperature

The stress tensor in turbulent flow

Equation 3.4.7 can be written in tensor form as

$$\rho\frac{D\overline{u_\iota}}{Dt}=F_i-\frac{\partial\bar{p}}{\partial x_i}+\mu\Delta\overline{u_\iota}-\rho\left(\frac{\partial\overline{u_\iota u_J}}{\partial x_i}\right) \quad 3.4.13$$

Where $\mu\Delta\overline{u_\iota}-\rho\left(\frac{\partial\overline{u_\iota u_J}}{\partial x_i}\right)=\mu\frac{\partial}{\partial x_j}\left(\frac{\partial u_\iota}{\partial x_j}\right)-\rho\frac{\partial}{\partial x_j}\overline{u_\iota u_J}=\frac{\partial}{\partial x_j}\left(\mu\frac{\partial u_i}{\partial x_j}-\overline{\rho u_\iota u_J}\right)$

The term in brackets in the above equation is known as total shear stress expressed as τ_{ij}.

Equation 3.4.7 can be written as

$$\rho \frac{D\overline{u_i}}{Dt} = F_i - \frac{\partial \bar{p}}{\partial x_i} + \frac{\partial}{\partial x_j}\tau_{ij} \qquad 3.4.14$$

With the approach of Eddy viscosity principle, equation 3.4.14 is referred as Reynods Averaged Navier Stokes equation (RANS).

and

$$\tau_{ij} = \mu \frac{\partial u_i}{\partial x_j} + \rho \left(V_T \left(\frac{\partial u_i}{\partial x_j} + \frac{\partial u_j}{\partial x_j} \right) - \frac{2}{3} k \delta_{ij} \right) \qquad 3.4.15$$

Where δ_{ij} is kronecker delta function

V_T is turbulent eddy viscosity

3.5 Approach of Boussinesq

A relative old approach to this principle of eddy viscosity, which in 1877 was formulated by Boussinesq and is still the basis of many turbulence models (Rodi 1993).

$$-\overline{u_i' u_j'} = V_T \left(\frac{\partial u_i}{\partial x_j} + \frac{\partial u_j}{\partial x_i} \right) - \frac{2}{3} k \delta_{ij} \qquad 3.4.16$$

Where *k* is kinetic energy turbulence defined as

$$k = \frac{1}{2}\left(\overline{u^2} + \overline{v^2} + \overline{w^2}\right) \qquad 3.4.17$$

Turbulent eddy viscosity, V_T depends on the degree of turbulence i.e. it varies within the fluid flow and depending on the flow condition. The approach of calculating eddy viscosity V_T is known as turbulence modelling.

Applications and approaches for turbulence modelling

The zeroth models, following the approach of Boussinesq (1877) assume that flow of velocity is proportional to turbulent stresses. In one equation model additional partial differential equation for velocity scale is used for turbulence. Another partial differential equation for length scale is added for two equation models. This group also includes $k-\varepsilon$ and $k-\omega$ models. Approaches to determine the turbulence eddy viscosity provides the described closer models zeroth, first and second order.

3.6 Shear Stress Transport $k-\omega$ model.

It is at two-equation eddy-viscosity model. It combines the standard and models. It activates model in the free stream and standard model near the wall. This makes sure that the suitable model is applied all through the stream field.

The transport equations of $k-\omega-SST$ model are;

$$\frac{\partial}{\partial t}(\rho k)+\frac{\partial}{\partial x_j}(\rho k u_i)=\frac{\partial}{\partial x_j}\left(\Gamma_k \frac{dk}{dx_j}\right)+\tilde{G}_k-Y_k+S_k$$

and

$$\frac{\partial}{\partial t}(\rho \omega)+\frac{\partial}{\partial x_j}(\rho \omega u_i)=\frac{\partial}{\partial x_j}\left(\Gamma_\omega \frac{d\omega}{dx_j}\right)+G_\omega-Y_\omega+S_\omega+D_\omega$$

$\tilde{G}_k=min\,(G_k, 10\rho\beta^* k\omega)$ - reproduction of turbulent kinetic energy owed to average velocity gradients where $G_k=-\rho\overline{u_j^{\prime}u_j^{\prime}}\frac{\theta u_j}{\partial x_i}$

$G_\omega=\frac{\alpha}{v_t}G_k$ is the generation of ω

D_ω denotes the cross-diffusion term.

Y_k and Y_ω denotes the dissipation of k and ω due to turbulence.

Γ_k and Γ_ω denotes the effective diffusivity of k and ω respectively.

For the $k-\omega-SST$ model, the effective diffusivities are given by

$\Gamma_k = \mu + \frac{\mu_i}{\sigma_k}$ and $\Gamma_\omega = \mu + \frac{\mu_i}{\sigma_\omega}$

where;

S_k and S_ω are user-defined source terms.

σ_ω and σ_k are turbulent prandtl numbers for ω and k correspondingly.

Constants are determined from experiment and their values are as per the table 3.1 below.

Table 3.1: Turbulence model constants

$\sigma_k,1$	1.176
$\sigma_\omega,1$	2.0
$\sigma_k,2$	1.0
$\sigma_\omega,2$	1.168
α_1	0.31
$\beta_i,1$	0.075
$\beta_i,2$	0.0828
α_∞^*	1
α_∞	0.25
α_o	$\frac{1}{9}$
β_ω^*	0.09
R_β	8
R_k	6
R_ω	2.95
ξ^*	2.5
M_{to}	0.25

CHAPTER FOUR

4.1 Mathematical Formulation

In this study numerical simulation of turbulent natural convection within a rectangular enclosure is studied. The physical situation is illustrated by the figure below,

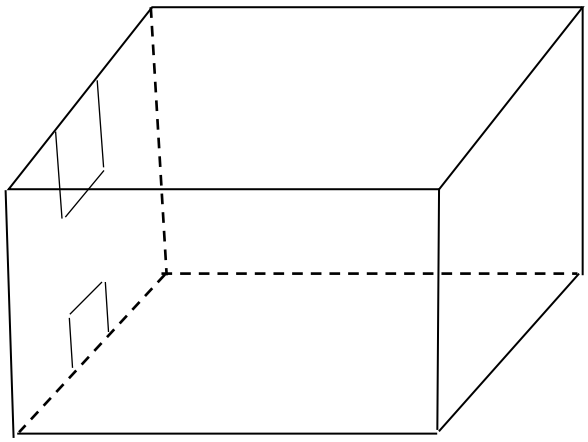

Fig. 4.1 Geometry of the problem

The cavity was maintained at 303K on a square hot section midway on the extreme lower boundary of one of the vertical walls and 283K on a square (twice in length and width the lower one) cold section midway on the extreme upper boundary on the same wall. The remaining part of this wall and the other five walls are adiabatic.

The fluid is initially motionless and at a uniform temperature equal to the average temperature of the vertical walls. The temperature of the hot section T_h and that of the cold section T_c is constant with $T_h > T_c$. Under this condition the density gradient of the internal fluid is normal to the gravity and the buoyancy –driven natural convection starts immediately when the heat is applied.

Due to buoyancy, a fluid motion is enclosed in the enclosure depending on the enclosure geometry (aspect ratio), the working fluid and the temperature difference .In this study, L=1m, W=$\frac{1}{2}$ and

D=0.32.The working fluid is air. Fluid flow therefore depends only on the temperature difference $dT = T_h > T_c$.In terms of dimensionless analysis, the presentative parameter is the geometrical aspect ratio. The aspect ratio is $A_x = \frac{l}{w} = \frac{2}{1}$ =2, $P_{r=} \frac{v}{\alpha}$ =0.72 and Ra =$\frac{g\beta\rho^2 c_p dt\, L^2}{\mu k}$

The temperature difference is chosen to give the Rayleigh number of interest. For this study Rayleigh number is varied from 10^{10} to 10^{13}.

The problem is to find the subsequent velocities and temperature as a function of time and position and the rate of heat transfer across an enclosure as a function of time. The third dimension is large enough so that the flow and heat transfer are two dimensional.

4.2 Set of Governing equations

The representing equations in two dimensional rectangular directions;

$$\frac{\partial u}{\partial x} + \frac{\partial v}{\partial y} = 0 \quad \text{..... 4.1}$$

$$\frac{\partial u}{\partial t} + u\frac{\partial u}{\partial x} + v\frac{\partial u}{\partial y} = F_X - \frac{\partial p}{\partial x} + \mu\left(\frac{\partial^2 u}{\partial x^2} + \frac{\partial^2 u}{\partial y^2}\right) \quad \text{.....4.2}$$

$$\frac{\partial v}{\partial t} + u\frac{\partial v}{\partial x} + v\frac{\partial v}{\partial y} = F_y - \frac{\partial p}{\partial y} + \mu\left(\frac{\partial^2 v}{\partial x^2} + \frac{\partial^2 v}{\partial y^2}\right) \quad \text{.....4.3}$$

$$\rho C_P\left(\frac{\partial T}{\partial t} + u\frac{\partial T}{\partial x} + v\frac{\partial T}{\partial y}\right) = k\left(\frac{\partial^2 T}{\partial x^2} + \frac{\partial^2 T}{\partial y^2}\right) + \Phi \quad \text{.....4.4}$$

Where

$$\Phi = \mu\left\{2\left[\left(\frac{\partial u}{\partial x}\right)^2 + \left(\frac{\partial v}{\partial y}\right)^2\right] + \left(\frac{\partial v}{\partial x} + \frac{\partial u}{\partial y}\right)^2\right\}$$

These conditions are legitimate for the present issue; despite that, density is a component of temperature. To change over the issue into an even state, Boussinesq estimation is usually utilized. Boussinesq estimation for limit layer streams and the current issue are depicted in the following two segments.

4.3 Limit Layer Stream Boussinesq Approximations

As constrained convection, the conditions that portray energy and momentum move in the convection starts from linked conservation ideologies. The distinction among the two streams is that buoyancy forces play a noteworthy part in free convection. It such powers that, truth be told, maintain the stream (Incropera and Dewitt 2002).

Adopting uneven, 2 – D, consistent property circumstances where force of gravity act in the negative y course. Likewise, with one exemption, accept the liquid to be incompressible. The special case that initiates fluid movement. The last supposition is that the approximations of limit layer are with consistent properties, y-momentum eqn 4.3 decreases to the limit layer eqn 4.5, apart from is made by gravity, the body force for each unit volume is $f_y = -g$, with g as the neighborhood increasing speed because of gravity. Boussinesq estimation say that at every term of the equation of momentum, with exception of the body constrain term, density is steady.

At that point, $\rho = \rho(T)$ for the body force.

$$\rho\frac{\partial v}{\partial t} + \rho u\frac{\partial v}{\partial x} + \rho v\frac{\partial v}{\partial y} = \rho g - \frac{\partial p}{\partial y} + \mu\left(\frac{\partial^2 v}{\partial x^2} + \frac{\partial^2 v}{\partial y^2}\right) \quad \text{.....4.5}$$

Equation 4.5 might be framed in a more suitable method by first taking note of that from the x-momentum equation 4.2, $\frac{\partial p}{\partial x} = 0$ if there is no body force in x-course which implies no pressure change toward a path perpendicular to the surface. Henceforth the y-pressure slope anytime in the limit layer must be equivalent to the pressure inclination. Be that as it may, in this locale $v = 0$ and the Eqn 4.5 diminishes to;

$$\frac{\partial p}{\partial y} = -\rho_\infty g \quad \text{.....4.6}$$

By substituting Eqn 4.6 into 4.5, resulting equation for momentum in y-course is acquired after executing some mathematical operations.

$$\frac{\partial v}{\partial t} + u\frac{\partial v}{\partial x} + v\frac{\partial v}{\partial y} = g\left(\frac{\Delta\rho}{\rho}\right) + \mu\left(\frac{\partial^2 v}{\partial x^2} + \frac{\partial^2 v}{\partial y^2}\right) \quad \text{.....4.7}$$

Where $\Delta\rho = \rho_\infty - \rho$ and this applies at each section in the unrestricted convection limit layer. On the RHS of eqn 4.7, buoyancy force is the first term and stream begin on the ground that density ρ is adjustable. In the event that variations of destiny are just owed to variations of temperature, the term might be associated to property of a fluid identified as coefficient of volumetric thermal expansion which is;

$$\beta \approx -\frac{1}{\rho}\left(\frac{\Delta\rho}{\Delta T}\right) \quad \text{.....4.8}$$

It gives a measure of the quantity by which the density change at steady pressure due to variation of temperature. It's stated in the estimated formula below;

$$\beta \approx -\frac{1}{\rho}\left(\frac{\Delta\rho}{\Delta T}\right) = -\frac{1}{\rho}\frac{\rho_\infty - \rho}{T_\infty - T} \quad \text{.....4.9}$$

It takes after that

$$\rho_\infty - \rho \approx \rho\beta(T_\infty - T) \quad \text{.....4.10}$$

This interpretation is identified as Boussinesq estimate and replacing it into Eqn 4.5, the y-momentum equation becomes;

$$\frac{\partial v}{\partial t} + u\frac{\partial v}{\partial x} + v\frac{\partial v}{\partial y} = g\beta(T_\infty - T) + \mu\left(\frac{\partial^2 v}{\partial x^2} + \frac{\partial^2 v}{\partial y^2}\right) \quad \text{.....4.11}$$

Where it's presently clear how the buoyancy force, which drives the stream. The Boussinesq estimate is applied in natural convection in fluid dynamics which state that differences in density are adequately little to be disregarded, aside from where they show up as multiples of g (gravitational acceleration).

4.4 Boussinesq Approximation for the Considered Issue

For this work, there is not any of the body force in x-course and gravitational force g is the body force acting in negative y-course. If density varies just because of temperature differences (p=constant), Boussinesq estimation can be used into y-momentum eqn 4.5 by bearing in mind the dynamic and static pressures;

$$\rho\frac{\partial v}{\partial t}+\rho u\frac{\partial v}{\partial x}+\rho v\frac{\partial v}{\partial y}=-\frac{\partial pdynamic}{\partial y}+\mu\left(\frac{\partial^2 v}{\partial x^2}+\frac{\partial^2 v}{\partial y^2}\right)-\frac{\partial pstatic}{\partial y}-\rho g \quad \text{.....4.12}$$

By introducing 4.10 into 4.12

$$\rho\frac{\partial v}{\partial t}+\rho u\frac{\partial v}{\partial x}+\rho v\frac{\partial v}{\partial y}=-\frac{\partial pdynamic}{\partial y}+\mu\left(\frac{\partial^2 v}{\partial x^2}+\frac{\partial^2 v}{\partial y^2}\right)+\rho_\infty g-\rho g \quad \text{.....4.13}$$

Equation 4.13 can be rearranged to get $\rho_\infty g-\rho g$

$$\rho\frac{\partial v}{\partial t}+\rho u\frac{\partial v}{\partial x}+\rho v\frac{\partial v}{\partial y}=-\frac{\partial pdynamic}{\partial y}+\mu\left(\frac{\partial^2 v}{\partial x^2}+\frac{\partial^2 v}{\partial y^2}\right)+g(\rho_\infty-\rho) \quad \text{.....4.14}$$

And by using the relation 4.10 in 4.14, following can be obtained;

$$\rho\frac{\partial v}{\partial t}+\rho u\frac{\partial v}{\partial x}+\rho v\frac{\partial v}{\partial y}=-\frac{\partial pdynamic}{\partial y}+\mu\left(\frac{\partial^2 v}{\partial x^2}+\frac{\partial^2 v}{\partial y^2}\right)+pg\beta(T_\infty-T) \quad \text{.....4.15}$$

The Boussinesq assumptions made in this study (Boussinesq, 1903) include:

- All the fluid motion transport properties remain constant apart from density in the buoyancy term.
- The characteristic temperature ΔT be sufficiently small i.e. it tends to zero.
- The viscous dissipation effect is negligible.
- The density varies linearly with temperature and the derivation from a reference value ρ_z is sufficiently small.

4.5 Dimensionless Energy, Momentum and Continuity Equations

Non-dimensional zing governing equations simpler and highlights which terms are the most important. The main objective behind non-dimensionalization is to lessen number of variables.

The set of Equations 4.1, 4.2, 4.3 and 4.4 ought to be resolved to acquire the unknowns p, v, T and u. By applying Boussinesq estimation and then bringing up dimensionless constraints P, V, U, r, θ, Y and X;

$$X = \frac{x}{L}, Y = \frac{y}{L}, U = \frac{uL}{\alpha_f}, V = \frac{vL}{\alpha_f}, \theta_f = \frac{T_f - T_c}{T_h - T_c}, \tau = \frac{\alpha_f t}{L^2}, p = \frac{L^2 \rho}{\rho \alpha^2 f} \quad \text{.....4.16}$$

The set of equation in dimensionless form becomes:

$$\frac{\partial U}{\partial X} + \frac{\partial V}{\partial Y} = 0 \quad \text{..... 4.17}$$

$$\frac{\partial U}{\partial \tau} + U\frac{\partial U}{\partial X} + V\frac{\partial U}{\partial Y} = -\frac{\partial P}{\partial X} + Pr\left(\frac{\partial^2 U}{\partial X^2} + \frac{\partial^2 U}{\partial Y^2}\right) \quad \text{.....4.18}$$

$$\frac{\partial V}{\partial \tau} + U\frac{\partial V}{\partial X} + V\frac{\partial V}{\partial Y} = -\frac{\partial P}{\partial Y} + Pr\left(\frac{\partial^2 V}{\partial X^2} + \frac{\partial^2 V}{\partial Y^2}\right) + Ra.Pr.\theta_f \quad \text{.....4.19}$$

$$\left(\frac{\partial \theta_f}{\partial \tau} + U\frac{\partial \theta_f}{\partial X} + V\frac{\partial \theta_f}{\partial Y}\right) = k\left(\frac{\partial^2 \theta_f}{\partial X^2} + \frac{\partial^2 \theta_f}{\partial Y^2}\right) + \phi \quad \text{.....4.20}$$

Where, Pr and Ra denotes Prantdl and Rayleigh numbers correspondingly; and θ_f is the dimensionless fluid temperature. In the next section, Grashof, Prandtl and Rayleigh number will be defined.

4.6 Dimensionless Constraints

4.6.1 Prandtl Numbers

Is a proportion of the momentum diffusivity to thermal diffusivity $\propto$

$$Pr = \frac{V}{\alpha^2} \quad \text{.....4.21}$$

It give a degree of the comparative efficiency of energy and momentum transport by diffusion in the speed and thermal limit layers. When Prandtl value is near to 1, then the momentum and energy transmission by diffusion are equivalent. If it's less than 1, momentum diffusion rate is significantly exceeds by energy diffusion rate. The inverse is valid for Prandtl numbers more than

1. This shows that Prandtl value greatly effects the relative development of velocity and thermal limit sheets.

4.6.2 Grash of Number

Is the dimensionless number defined as;

$$Gr_l = \frac{g\beta(T_s - T_\infty)L^3}{V^2} \quad \text{.....4.22}$$

The Grashof number assumes a comparable part in free convection that Reynolds number play in constrained convection. The measure of proportion of inertia to viscid forces acting on a fluid components given by Reynolds number. Conversely, Grashof value shows the proportion of buoyancy forces to viscid force acting on the fluid.

4.6.3 Rayleigh Number

Noting that free convection limit layers aren't confined to laminar stream. Free convection streams ordinarily begin from a thermal unsteadiness i.e. hotter and less dense fluid rises upwards with respect to cooler and denser fluid. Nonetheless, for forced convection, hydrodynamic variabilities may likewise emerge. I.e., instabilities in the stream might be increased, prompting progress to turbulent from laminar stream. Change in free convection limit layers relies upon the relative size of viscid and buoyancy forces in the fluid. It is standard to correspond its event as far as the Rayleigh, which is basically the result of Prandtl and Grashof number;

$$Ra_L = Gr_l Pr = \frac{g\beta(T_S - T_\infty)L^3}{v^\propto} \quad \text{.....4.23}$$

The critical Rayleigh number for vertical plates is 10^8. Around this number shift to turbulence starts. According to Incropera and Dewitt (2002), trubulence strongly affects heat transmission

that is why great importance is set on trial outcomes to get suitable correlations for turbulence stream where Rayleigh value is larger than 10^9.

4.7. Two Dimensional Flow vorticity definition

(Aksel 2003) defines vorticity vector, $\vec{\xi}$, as curl speed vector, $\vec{V}$;

$$\vec{\xi} = curl\vec{V} = \nabla \times \vec{V} \quad \text{.....4.29}$$

For two-dimensional stream, Eqn 4.29 becomes;

$$\xi = \frac{\partial u}{\partial x} - \frac{\partial v}{\partial y} \quad \text{.....4.30}$$

All through the turning, the course of a fluid component changes however its location, shape and dimensions don't change. At the point when the liquid component moving in a stream field does not experience any pivot, at that point the stream is known to be irrotational. For irrotational stream;

$$\vec{\xi} = curl\vec{V} = \nabla \times \vec{V} = 0$$

4.8. Stream function - Vorticity Relation and Vorticity Transport Equation

Differentiating dimensionless y-momentum eqn 4.19 w.r.t X and dimensionless x-momentum eqn 4.18 w.r.t Y, eqn. 4.32 is arrived at after eliminating the dimensionless pressure term P by rearranging the derivatives;

$$\frac{\partial}{\partial \tau}\left(-\frac{\partial U}{\partial Y} + \frac{\partial V}{\partial X}\right) + U\frac{\partial}{\partial X}\left(-\frac{\partial U}{\partial Y} + \frac{\partial V}{\partial X}\right) + V\frac{\partial}{\partial X}\left(-\frac{\partial U}{\partial Y} + \frac{\partial V}{\partial X}\right) = Pr\left[\left(\frac{\partial}{\partial X}\right)^2\left(-\frac{\partial U}{\partial Y} + \frac{\partial V}{\partial X}\right) + \left(\frac{\partial}{\partial Y}\right)^2\left(-\frac{\partial U}{\partial Y} + \frac{\partial V}{\partial X}\right)\right] + RaPr\frac{\partial \theta_f}{\partial X} \quad \text{.....4.32}$$

The dimensionless vorticity can be defined as;

$$\frac{\partial V}{\partial X} - \frac{\partial U}{\partial Y} = \Omega \quad \text{.....4.33}$$

After introducing the dimensionless vorticity 4.33 into Equation 4.32;

$$\frac{\partial \Omega}{\partial \tau} + U\frac{\partial \Omega}{\partial X} + V\frac{\partial \Omega}{\partial Y} = Pr\left(\frac{\partial^2 \Omega}{\partial X^2} + \frac{\partial^2 \Omega}{\partial Y^2}\right) + RaPr\frac{\partial \theta_f}{\partial X} \quad \text{.....4.34}$$

Equation 4.34 is the vorticity transport condition. In the x and y momentum, the pressure term is eliminated thus reducing the two equations to one. The dimensionless stream function can be defined as

$$U = \frac{\partial \psi}{\partial Y} and\ V = -\frac{\partial \psi}{\partial X} \quad \text{.....4.35}$$

$$\frac{\partial U}{\partial Y} = \frac{\partial^2 \psi}{\partial Y^2} and\ \frac{\partial V}{\partial Y} = -\frac{\partial^2 \psi}{\partial X^2} \quad \text{.....4.36}$$

From the definition of dimensionless vorticity 4.33 and by using 4.36;

$$\frac{\partial^2 \psi}{\partial X^2} + \frac{\partial^2 \psi}{\partial Y^2} = -\Omega \quad \text{.....4.37}$$

Equation 4.37 is the equation of stream function that's demonstrating the connection between dimensionless stream function and dimensionless vorticity.

4.9. Equation Sets in Stream function-Vorticity Form

By utilizing dimensionless stream function 4.35 and dimensionless vorticity 4.33 variables, eliminating pressure term in the equation of momentum, governing equations in dimensionless form are acquired. Using vorticity-stream function method, the resulting equations are used in finding unknown velocities and temperature values;

$$\frac{\partial \Omega}{\partial \tau} + \frac{\partial U\Omega}{\partial X} + \frac{\partial V\Omega}{\partial Y} = Pr\left(\frac{\partial^2 \Omega}{\partial X^2} + \frac{\partial^2 \Omega}{\partial Y^2}\right) + RaPr\frac{\partial \theta_f}{\partial X} \quad \text{.....4.38}$$

$$\frac{\partial^2\psi}{\partial X^2}+\frac{\partial^2\psi}{\partial Y^2}=-\Omega \quad \text{.....4.39}$$

$$\frac{\partial\theta_f}{\partial\tau}+\frac{\partial U\theta_f}{\partial X}+\frac{\partial V\theta_f}{\partial Y}=\frac{\partial^2\theta_f}{\partial X^2}+\frac{\partial^2\theta_f}{\partial Y^2} \quad \text{.....4.40}$$

In the equation 4.38, Rayleigh number is;

$$Ra=\frac{g\beta(T_h-T_c)L^3}{v^\infty} \quad \text{.....4.41}$$

and the dimensionless vorticity and stream function are 4.33 and 4.35, respectively.

Although the boundary conditions become relatively complicated in such an indirect method to solution of Navier - Stokes equations, the vorticity - stream formulation is more attractive than the primitive variable formulation because:-

i. The number of differential equations to be solved is reduced.

ii. Continuity equation is automatically satisfied.

iii. It does not require staggered finite difference grid systems.

4.10 Boundary Conditions

The parameters of the approaching stream (dissipation of the turbulent kinetic energy o, stream velocity or pressure and turbulent kinetic energy k) are viewed as known. The limit conditions suggested are:

$$\frac{U_\infty}{L}<\omega farfield<10\frac{U_\infty}{L}$$

$$\frac{10^{-5}U_\infty^2}{ReL}<kfarfield<\frac{0.1U_\infty^2}{ReL}$$

$$\omega_{wall}=10\frac{6v}{\beta_1(\Delta d_1)^2}$$

$$k_{wall} = 0$$

Where L is the approximate length of computational area

In this study, temperature of the hot wall was kept at 303K and the other cold wall at283K.

The operating temperature inside the enclosure of the air is 293K.

The Rayleigh number of the enclosure varied from $10^{10}, 10^{11}, 10^{12}$ and 10^{13}

4.11 The $k - \omega$ Model of Turbulence

This is one of the frequently utilized turbulence models. This lets a two - equation model to justify for history Impacts such as diffusion of turbulent energy and convection. For this work, the $k - \omega - SST$ Model will be utilized. According to Menter (1993), the utilization of $k - \omega$ formulation in the internal sections of the limit layer makes the model straightforwardly usable all the way down to the wall through the viscid sub-layer, hence the $k - \omega - SST$ model can be utilized as a low re-turbulence model with no additional damping function.

Thus, it was resolved that the $k - \omega - SST$ model ought to be authenticated.

4.12 Buoyancy - driven and Natural Convection Flows

When a fluid heated and its density change with temperature a stream can be brought by gravitational force acting on the density differences. Such buoyancy - driven streams are called natural convection (or mixed - convection) streams and can be modeled by FLUENT.

4.13 Low - Reynolds Number Models

Turbulent unrestricted convection from a heated vertical wall is predicted using the standard forced stream modification by Gatheri (1994), Lin and Churchill (1978) require the insertion of a destruction term.In the E- equation it is necessary to include a generation term $2vv\left(\frac{\partial^2 u_j}{\partial X^2{}_k}\right)^2$

C_u and $C_{\varepsilon 2}$ are made function of R_t, turbulence Reynolds Number of $R_t = \frac{k^2}{v\varepsilon}$ which accounts for the Low - Reynolds impact on the stream region. The variation of C_u is determined by necessitating that the turbulence viscosity change as per Van Driest design in the near wall region.

The variation of $C_{\varepsilon 2}$ is selected such that the model will correctly foresee the decay isotropic grid turbulence for both low and high turbulence intensities like in this case. Low - Reynolds number models are designed to maintain the high - Reynolds turbulence formulation in the Log - Law regions and fit measurement in the viscous sub - layer near walls. Parameters C_u and $C_{\varepsilon 2}$ are functions of Reynolds Number.

4.14 Boundary Conditions

4. 14.1 Temperature Boundary Conditions

The non - dimensional was defined by $\theta_f = \frac{T_f - T_c}{\Delta T}$ where $\Delta T.$ is the characteristic temperature variance between hot and cold surfaces i.e. $\Delta T. = T_h - T_c$ the choice of θ_f ensures that it is bounded and lie between 0 and 1. The thermal boundary conditions which were used are isothermal and adiabatic conditions. These conditions are represented by the equations:

$$\theta_f = constant$$

$$\frac{\partial \theta_f}{\partial n} = 0$$

Where n represents the direction perpendicular to a wall. Since the problem involves heating on one wall and cooling on the opposite wall all the remaining four walls of the enclosure are kept adiabatic on the cold and hot walls, the Derichlet boundary conditions are used where

$$\theta_{hot} = 1 \; and \; \theta_{cold} = 0$$

Neumann boundary condition is used on the remaining four walls i.e. $\frac{\partial \theta_f}{\partial n} = 0$ for each of four walls.

4. 14.2 Velocity Boundary Conditions

The conditions in the motion of fluid at a boundary are specified in terms of the velocity. Particles close to a surface do not move along with a flow when adhesive forces are stronger than cohesive forces. In a closed cavity each boundary is impermeable. Normal component of velocity at each boundary is zero. For example, the boundary x=0 in the $y - z$ plane. The velocity component orthogonal to the surface is certainly zero as mass can't penetrate an impermeable solid surface.

The differential equations are solved by means of Fluent 6.3.26 program. The results obtained are presented and discussed in the next chapter. Recommendations on other areas that can be investigated were also given.

CHAPTER FIVE

NUMERICAL METHOD

5.1 Introduction

Fluid movement is guided by Navier Stokes equations, a set of nonlinear and coupled PDEs resulting from basic laws of conservation of energy, momentum and mass. The unknowns are generally temperature, pressure, stream velocity and density. The analytical solution of these equations is not possible henceforth in such situations, scientists resort to laboratory experiments. The results are generally qualitatively not the same as geometric and dynamical similitude are hard to apply at the same time between the laboratory experiment and prototype. Moreover, the plan and creation of these experimentations can be hard and expensive, especially for stratified spinning streams. Computational fluid dynamics (CFD) is a supplementary tool in the collection of scientists. Is a branch of fluid mechanics that uses data structures and numerical analysis to solve and analyze issues that involve fluid streams. Computers are utilized to play out the estimations necessary to simulate the interaction of fluids with surfaces defined by limit situations. Earlier, CFD was frequently contentious, as it included extra estimation to governing equations and brought up authentic problems. These days CFD is a well-known discipline along with experimental and theoretical approaches. This position is in substantial part because of the exponential development of PC control which has enabled us to handle ever bigger and more compound issues.

In CFD, the fundamental procedure is discretization. It's the way toward taking differential equations with unlimited amount of degrees of freedom and minimizing them to a limited degrees of freedom system. Subsequently, rather than solving all over and for all times, we will be contented with its calculation at definite time intervals and at limited number of locations. The

partial differential equations are then decreased into an arrangement of arithmetic equations that can now be resolved. To guarantee that correct equations are being solved and that there is stability and convergence, there must be control of nature and characteristics of errors that may arise during the process of discretization process. Several discretization methods have been established to handle a variety of issues. They are spectral, finite volume, finite element and finite difference methods. We shall use finite difference methods for the purpose of this work.

5.2 Finite Difference Solution Method

It allows the dependent parameter values of a certain differential equation at all separate points in the computational area to be determined. The method employs the Taylor series expansion in writing the derivative of a parameter as the difference among values of the parameter at several points in time or space.

Fig 5.1 shows a curve of u against x, i.e. $u(x)$. After discretization, the curve $u(x)$ can be represented by a set of separate points, $u's$ where Taylor series expansion can be used to relate them to each other. Considering a small change Δx from point (i) for points $(i-1)$ and $(i+1)$.

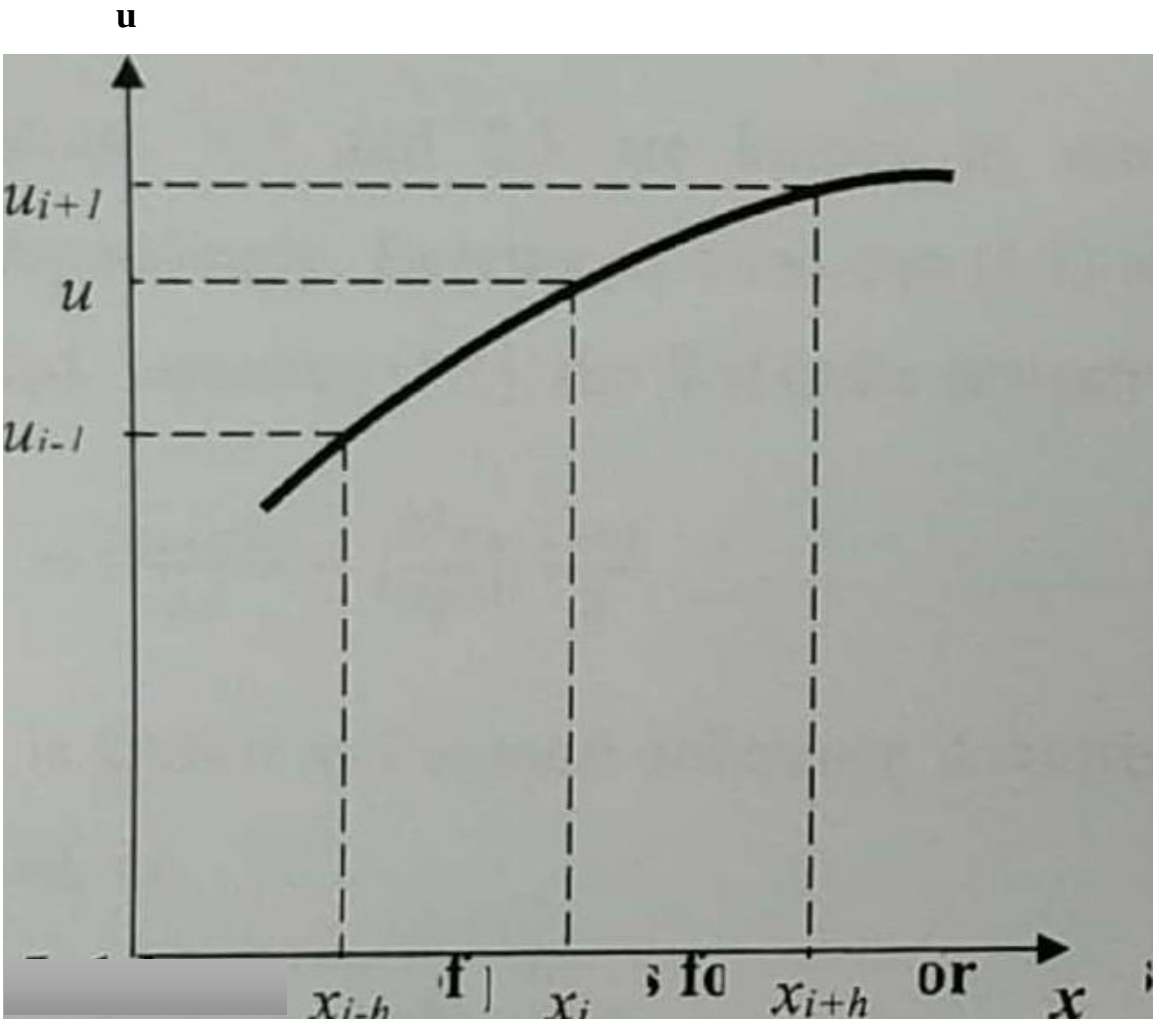

Fig. 5.0 Location of points for Tailor's series expansion.

Using Taylor series expansion about point(i), the velocity u_i can be expressed as:

$$u_{i+1} = u_i - \left[\frac{\partial u}{\partial x}\right]\Delta x + \frac{\partial^2 u}{\partial x^2}\frac{(\Delta x)^2}{2} + \left[\frac{\partial^2 u}{\partial x^3}\right]_i \frac{(\Delta x^3)}{6} + \ldots\ldots\ldots\ldots\ldots\ldots\ldots\ldots\ldots\ldots\ldots\ldots\ldots\ldots 5.1$$

And

$$u_{i-1} = u_i - \left[\frac{\partial u}{\partial x}\right]\Delta x + \frac{\partial^2 u}{\partial x^2}\frac{(\Delta x)^2}{2} + \left[\frac{\partial^2 u}{\partial x^3}\right]_i \frac{(\Delta x^3)}{6} + \ldots\ldots\ldots\ldots\ldots\ldots\ldots\ldots\ldots\ldots\ldots\ldots\ldots\ldots 5.2$$

If Δx is little and number of terms are unlimited, then the above equations are numerically correct.

Overlooking these terms prompts to a basis of error in the mathematical calculations as the

equation for the derivatives is truncated and the error is known as truncation error. The truncation error for the second order accurate is expressed as:

$$\sum_{n=3}^{\infty}\left[\frac{\partial^n u}{\partial x^n}\right]_i \frac{(\Delta x)^{n-1}}{n!} \quad \text{.....5.3}$$

By subtraction or addition of eqns 5.1 and 5.2, the first and second derivatives at the central position i can be found. They are

$$\left[\frac{\partial u}{\partial x}\right]_i = \frac{u_{i+1}-u_{i-1}}{2\Delta x} - \left[\frac{\partial^2 u}{\partial x^3}\right]_i \frac{\left(\Delta x^3\right)^2}{6} \quad \text{.....5.4}$$

And

$$\left[\frac{\partial u}{\partial x}\right]_i = \frac{u_{i+1}-u_{i-1}}{(\Delta x)^2} + o(\Delta x)^2 \quad \text{.....5.5}$$

Equations 5.4 and 5.5 are known as central difference for first and second derivative, correspondingly. Bearing in mind eqn (5.1) and (5.2) in isolation, more derivatives can also be formed. Equation (5.1), the first order derivative can be formed as

$$\left[\frac{\partial u}{\partial x}\right]_i = \frac{u_{i+1}-u_i}{\Delta x} - \left[\frac{\partial^2 u}{\partial x^2}\right]_i \frac{(\Delta x)}{2} \quad \text{.....5.6}$$

This is known as Forward difference. Likewise, from eqn (5.2) another-order derivative can be formed, i.e.

$$\left[\frac{\partial u}{\partial x}\right]_i = \frac{u_i-u_{i-1}}{\Delta x} - \left[\frac{\partial^2 u}{\partial x^2}\right]_i \frac{(\Delta x)}{2} \quad \text{.....5.7}$$

This is referred as backward difference.

The distinguishing feature of a Finite Difference Method is estimation of the temporal $\frac{\partial \emptyset}{\partial t}$ and spatial $\left(\frac{\partial^2 \emptyset}{\partial x^2}, \frac{\partial^2 \emptyset}{\partial y^2}\right)$ partial derivative in the governing equation with finite difference relating the

values of the unidentified functions at a set of bordering grid points at several time-levels. Due to this approximation Partial Differential Equation (PDE) is replaced by the Finite-Difference Equation (FDE). The process of replacing the Partial Differential Equation with an algebraic Finite-Difference Equation is called Finite-Difference discretization or approximation.

Process of Finite-Difference discretization is done in two steps, namely discretization of the solution domain and discretization of governing equations.

5.3 Discretization of the Solution Domain

The stream in turbulent natural convection in an enclosure is characterized by a thin limit layer along the walls while the core is thermally stratified. A large quantity of grid points or computational nodes are required since the stream gradient is great in the limit layer, where the values of dependent parameters should be determined. In this study the primitive variable is used hence there is no need for a staggered finite difference grid system. The domain of the solution i.e., the enclosure is partitioned into a network of uniform rectangular grid with very fine spacing.

Figure 5.2 illustrates a 2-D computational area in Cartesian coordinate framework divided into small areas. The center to each subdivided area is a reference point called the node. There are four neighboring nodes for each node (i, j) in a 2-D computational area as shown in Fig. 5.3.

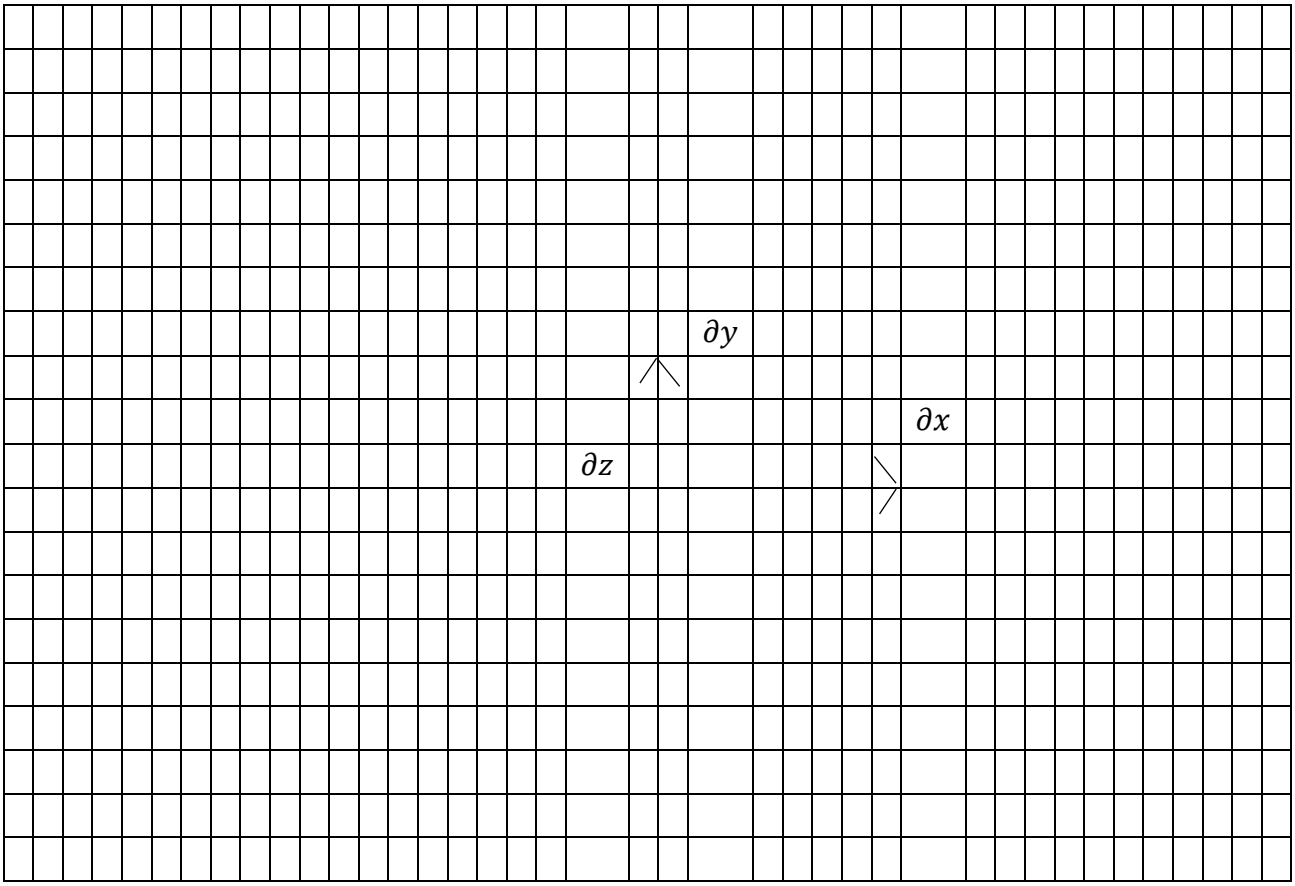

Fig. 5. 2 A two-dimensional Computational grid.

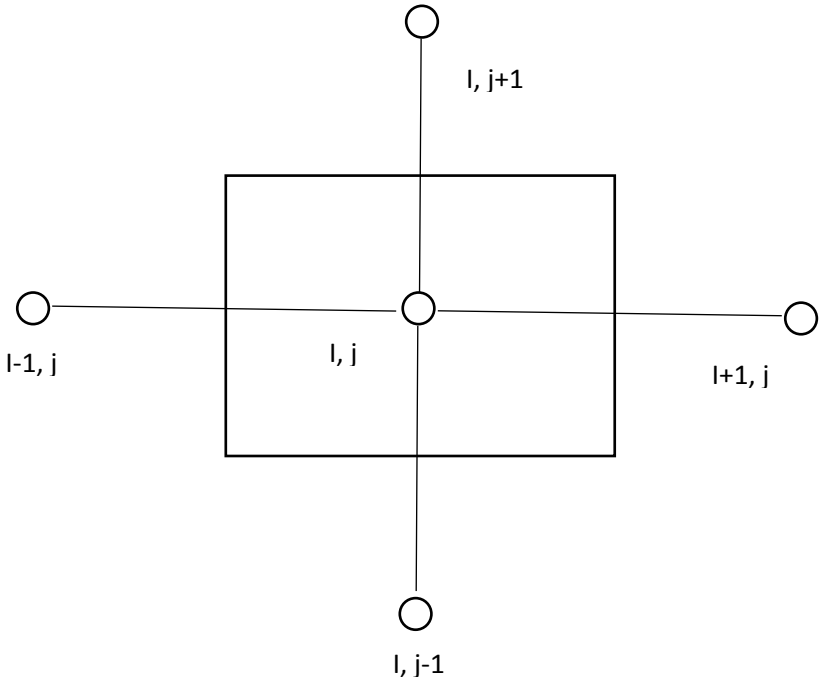

Fig. 5. 3 Cartesian coordinate showing a node (i,j) with its bordering nodes

5.4 Discretization of Governing Equations

This involves replacing governing equations with a finite-difference equation which is then applied sequentially at the internal nodes of the grid to give system of linear arithmetic equations that relate the estimation of unknown function θ at the nodes.

The goal of PDE with the FDE is to generate the estimations of the function θ at the nodes (i, j).

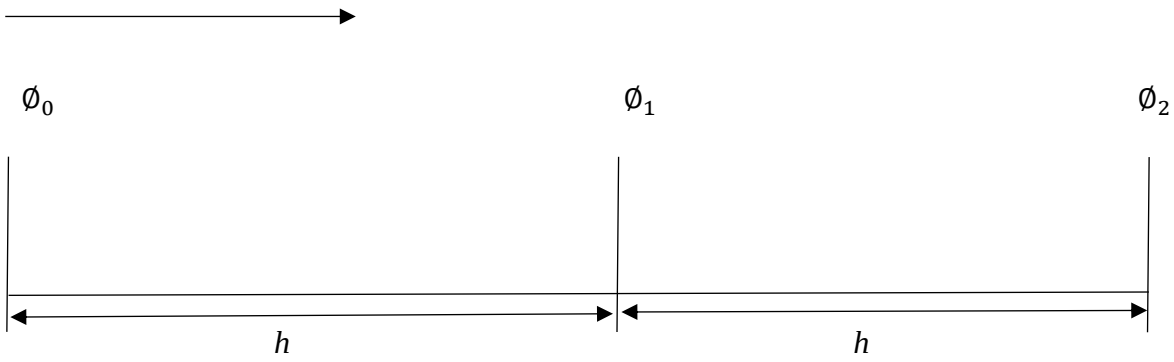

Fig. 5. 4 Three point Difference Approximation

$$\emptyset_2 = \emptyset_1 + h\emptyset' + \frac{h^2}{2}\emptyset'' + \frac{h^3}{6}\emptyset''' + 0(h^4) \quad \text{……..5.8}$$

$$\emptyset_0 = \emptyset_1 + h\emptyset' + \frac{h^2}{2}\emptyset'' - \frac{h^3}{6}\emptyset''' + 0(h^4) \quad \text{……..5.9}$$

Subtracting equation (5.9) from (5.8) yields

$$\emptyset_2 - \emptyset_0 = 2h\emptyset' + \frac{1}{3}h\emptyset''' + o(h^4) \quad \text{…….5.10}$$

Rearranging equation (5.10) we get

$$\emptyset' = \frac{\emptyset_2 - \emptyset_0}{2h} + o(h^4) \quad \text{……..5.11}$$

Adding equation (5.8) and (5.9) gives

$$\emptyset_2 + \emptyset_0 = 2\emptyset_1 + h^2\emptyset'' + o(h^4) \quad \text{…….5.12}$$

Rearranging the above equation results to

$$\emptyset'' = \frac{\emptyset_2 - 2\emptyset_1 - \emptyset_0}{h^2} + o(h^2) \quad \text{……...5.13}$$

Where h is the grid spacing.

Now, using Taylor series expansion in *t* to approximate the derivative of time $\frac{\partial \emptyset}{\partial t}$ with first order backward difference method about a node (i, j) at time instant t^{n+1} we get

$$\frac{\partial \emptyset}{\partial t} = \frac{\emptyset_{i,j}^{n+1} - \emptyset_{i,j}^{n}}{\Delta t} + o(\Delta t) \quad \text{.....5.14}$$

Using Taylor series expansion to approximate spatial derivatives with second order centered difference, we get

$$\frac{\partial^2 \emptyset}{\partial x^2} = \frac{\emptyset_{i-1,j}^{n+1} - 2\emptyset_{i,j}^{n+1} + \emptyset_{i+1}^{n+1}}{\Delta x^2} + o(h^2) \quad \text{.....5.15}$$

And

$$\frac{\partial^2 \emptyset}{\partial y^2} = \frac{\emptyset_{i,j-1}^{n+1} - 2\emptyset_{i,j}^{n+1} + \emptyset_{i+1}^{n+1}}{\Delta y^2} + o(h^2) \quad \text{.....5.16}$$

The method above gives second order accuracy in spatial partial derivatives and first order accuracy in time.

Finite difference method allows spatial derivative of a differential equation for a grid point *(i, j)* to be written in terms of dependent variable values at that grid point and its neighboring grid points. Thus, the differential equation for point *(i, j)* can be diminished to an estimated arithmetic equation and the solution gives the dependent parameter value at point *(i, j).*

Likewise, discretization in time of the problem is necessary for us to attain the dependent parameter value of a differential equation that depends on time at any point in the computational area. Thus, time derivative of the differential equation ought to be in terms of values of dependent parameter and a time interval ought to be defined; for instance, toward the start and end moment of the time intervals. In this work, the superscript n denotes time dependence of dependent parameter.

5.6 Finite Difference Solution Technique for Parabolic Differential Equations

Since energy eqn 4.40 and the vorticity eqn 4.38 are alike, Mobedi (1994), they can be written in form of a single generic equation

$$\frac{\partial \emptyset}{\partial \tau} + U\frac{\partial \emptyset}{\partial X} + V\frac{\partial \emptyset}{\partial Y} = C\left(\frac{\partial^2 \emptyset}{\partial x^2} + \frac{\partial^2 \emptyset}{\partial y^2}\right) + f \quad \text{.....5.17}$$

Where $\emptyset$ is a generic dependent variable representing Ω.

Equation 5.17 can be reduced to the following form;

$$\frac{\partial \emptyset}{\partial \tau} = \delta_X^2 \emptyset + \delta_Y^2 \emptyset + f \quad \text{.....5.18}$$

In equation 5.18, $\delta_X^2 \emptyset \; and \; \delta_Y^2 \emptyset$ are

$$\delta_X^2 \emptyset = C\frac{\partial^2 \emptyset}{\partial x^2} - U\frac{\partial \emptyset}{\partial X} \quad \text{.....5.19}$$

$$\delta_Y^2 \emptyset = C\frac{\partial^2 \emptyset}{\partial Y^2} - V\frac{\partial \emptyset}{\partial Y} \quad \text{.....5.20}$$

Term $\delta_Y^2 \emptyset$ and $\delta_X^2 \emptyset$ denote convection and diffusion transport in Y and X direction correspondingly. Therefore, they can be referred as diffusion-convection terms. Several finite difference approaches can be used to solve the parabolic PDE. These approaches are commonly categorized into 3 categories, i.e., Alternating Direction Implicit (ADI), implicit and explicit approaches (Thiault 1985).

i. Explicit Methods:

When the method is applied on Eqn 5.18 for any point (i, j) in Cartesian coordinates when a simple forward difference for the time term is utilized can be expressed as;

$$\frac{\emptyset_{i,j}^{n+1} - \emptyset_{i,j}^{n}}{\Delta \tau} = \delta_X^2 \emptyset_{i,j}^{n} + \delta_Y^2 \emptyset_{i,j}^{n} + f_{i,j}^{n} \quad \text{.....5.21}$$

Where $\emptyset_{i,j}^{n}$ and $\emptyset_{i,j}^{n+1}$ denote the estimate of dependent parameter $\emptyset$ at node (i, j) at n^{th} and $(n+l)^{th}$ time steps, correspondingly. By taking the numerical spatial derivatives of dependent parameter in the preceding time step, n^{th} in Eqn 5.21 the unknown estimate of dependent parameter at point (i, j), $\emptyset_{i,j}^{n+1}$ can be found. Since values of the dependent parameter at all points of the computational area at n^{th} time step are identified, it's easy to determine the unknown $\emptyset_{i,j}^{n+1}$ in Eqn 5.21.

Propagation of the dependent parameter is done point by point in explicit method. According to Roach (1976), stability of the technique needs utilization of small-time interval or small grid dimensions which requires high PC storage and computational period.

ii. Implicit Method

Applying implicit technique wholly on eqn 5.18 for any point (i, j) in Cartesian coordinate, when a simple forward difference for time term is utilized, can be expressed as;

$$\frac{\emptyset_{i,j}^{n+1}-\emptyset_{i,j}^{n}}{\Delta\tau} = \delta_X^2\emptyset_{i,j}^{n} + \delta_Y^2\emptyset_{i,j}^{n} + f_{i,j}^{n} \quad \text{.....5.22}$$

In implicit technique, the spatial derivative of dependent parameter at the same time step determines the dependent parameter value at a new time step for a point (i, j), $\emptyset_{i,j}^{n+1}$. Therefore, m nodal equations must be acquired and solutions found so as the value of dependent parameter can be determine for a new time step in the computational area with m points. Thus, parabolic differential equation solution with implicit technique might be more complex compared to explicit technique.

Entirely implicit techniques are more required for computational fluid issues. According to Roach (1976), in entirely implicit techniques, in computational domain, propagation speed of dependent parameter is unlimited and thus becomes as genuinely stable techniques. Solutions can be acquired

for larger grid size or time interval compared to explicit techniques. Even though, implicit techniques are theoretically suitable for computational fluid issues, practically to get results solutions of large matrices must be performed.

iii. ADI method

The ADI method splits the finite difference equation into two, one having the x - direction and the other the y - direction. Every time step is divided into two sub-steps of equal duration $\frac{1}{2}\Delta t$ and approximating the spatial derivatives in a partially implicit manner while working sequentially and alternating in the x - and y – direction.

For computational fluid problems, ADI techniques are more suitable than implicit techniques. As an alternative of large matrices, they offer simple tri-diagonal matrices of wholly implicit technique. According to Roach (1976), the tri-diagonal matrices can simply be solved by using Thomas Algorithm technique without any repetition. Mostly in an ADI method, for 2-D issues, parabolic differential equation, the Y course remains explicit while the equation is solved implicitly in X course. Similarly, the equation is solved implicitly in Y course. Thus, ADI technique decreases a 2-D implicit technique to a progression of 1-D implicit techniques.

Additionally, majority of ADI techniques are unconditionally steady techniques which allow the solution of parabolic differential equations for large time-intervals and mesh sizes. The issue of this work 2-D, to eliminate large matrices to get higher order accuracy of the fully implicit technique us of ADI technique on equation 5.18 when simple forward difference for the time term is utilized for any point (*i*,*j*) in Cartesian coordinate may be expressed in 2 stages as

$$\emptyset_{i,j}^{n+\frac{1}{2}} - \emptyset_{i,j}^{n} = \delta_x^2 \emptyset_{i,j}^{n+\frac{1}{2}} + \delta_y^2 \emptyset_{i,j}^{n} + f_{i,j}^{n} \quad \text{………………………………….. (5.23)}$$

$$\frac{\emptyset_{i,j}^{n+1}-\emptyset_{i,j}^{n+\frac{1}{2}}}{\frac{\Delta T}{2}} = \delta_x^2\emptyset_{i,j}^{n+\frac{1}{2}} + \delta_y^2\emptyset_{i,j}^{n+\frac{1}{2}} + f_{i,j}^{n+\frac{1}{2}} \text{……………………………..….(5.24)}$$

Where equation 5.23 is explicit for y-course and implicit for x-course, solution of dependent parameter at a new time step $\left(n+\frac{1}{2}\right)^{th}$ for a point (*i*,*j*), $\emptyset_{i,j}^{n+1}$ relies upon spatial derivatives of dependent parameter at the similar time step for x-course and mathematical spatial derivatives of dependent parameter in the proceeding time step n^{th} for y-course. As a second step, the solution of dependent parameter at a new time step $(n+1)^{th}$ for point (*i*,*j*), $\emptyset_{i,j}^{n+1}$, relies on spartial derivatives of dependent parameter at similar time step for y-course and the mathematical spartial derivative of dependent parameter in the proceeding time step $\left(n+\frac{1}{2}\right)^{th}$ for y-course.

Eqn 5.23 can be organized as

$$\left(1-\frac{\Delta T}{2}\delta_x^2\right)\emptyset_{i,j}^{n+\frac{1}{2}} = \left(1+\frac{\Delta T}{2}\delta_y^2\right)\emptyset_{i,j}^{n} + \frac{\Delta T}{2}f_{i,j}^{n} \text{………………………5.25}$$

Similarly equation 5.24 can be arranged as

$$\left(1-\frac{\Delta T}{2}\delta_y^2\right)\emptyset_{i,j}^{n+1} = \left(1+\frac{\Delta T}{2}\delta_x^2\right)\emptyset_{i,j}^{n} + \frac{\Delta T}{2}f_{i,j}^{n+\frac{1}{2}} \text{……………………5.26}$$

As it can be seen, the most important benefit of ADI technique is that result of the equation can be found after two stages with regard to a fully implicit technique.

5.7 Solver Execution

From the computer program fluent 6.3.26 menu is laid out such that order of operation is generally left to right and using the menu to get the solution we

- Imported and scaled mesh file.
- Selected the physical models.
- Defines material properties.
- Prescribed operating conditions.
- Set solver controls.
- Set up convergence monitors.
- Computed and monitored the solution for convergence and accuracy.

5.8 Solution procedure overview

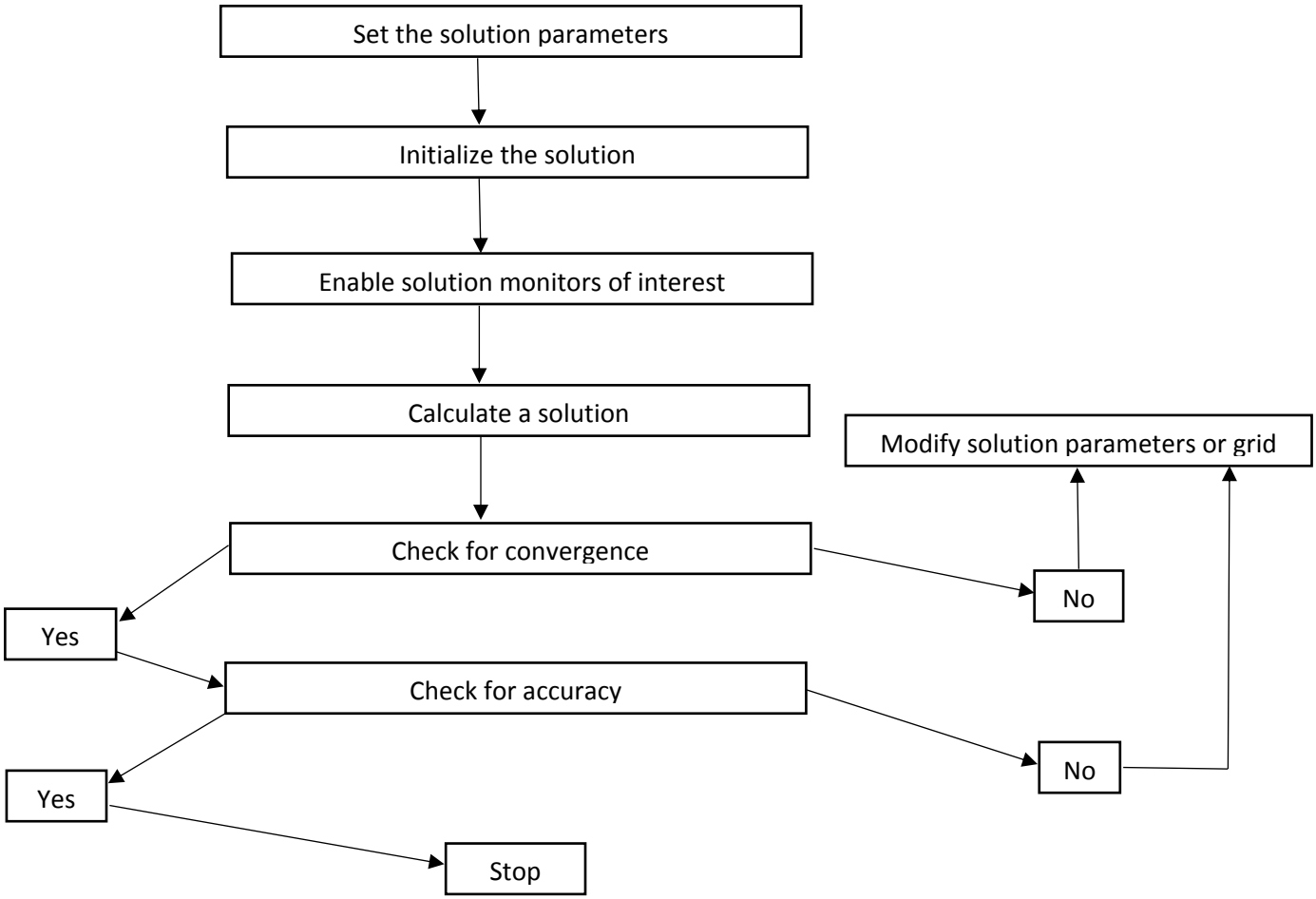

5.9 Turbulent flow important input

Table 5.1 shows the key input required to produce the outcomes shown in chapter six.

Table 5.1 Turbulent flow variable inputs.

Input	Value
Geometry	
Rayleigh number 10^{10}	2 by 1
Rayleigh number 10^{11}	4 by 2
Rayleigh number 10^{12}	8 by 4
Rayleigh number 10^{13}	18 by 9
Models	
Energy	On
Viscous	k-ω-SST
Material Properties (Air)	
Density	1.2047 kg/m^3
Dynamic Viscosity	$1.8205e-5\ kg/m.s$
Specific Heat Capacity	$1.0061e3\ J/kg.k$
Thermal conductivity	$0.025596\ w/m.k$
Thermal expansion coefficient	$3.4112e-3\ k^{-1}$
Solution Methods	
Pressure	PRESTO
Momentum	First Order Upwind
Turbulent Kinetic Energy	First Order Upwind
Turbulent Dissipation Rate	First Order Upwind

CHAPTER SIX

6.0 Results and discussion

The results presented here were obtained by resolving the governing equations mathematically by utilizing finite difference technique together with boundary conditions given the numerical solutions for variables in $k-\omega-SST$ model. In this study the results are obtained for different Rayleigh numbers i.e. $10^{10}, 10^{11}, 10^{12}, 10^{13}$ and results of isotherms streamlines and contours of velocity magnitude are recorded at $z = 0.5$.

6.1 Isotherms

Isotherm is a line of equal or constant temperature or is a curve on a graph that connects points of equal temperature. In the fig 6.11 the maximum temperature is 257K, in fig 6.1.2, the highest temperature is 249K, in 6.1.3, the highest temperature is 230K, and in 6.1.4, the highest temperature is 199K.

The high temperature are evident on the left side wall. In all cases two round motion in opposite directions (clockwise and anticlockwise direction). There is rising up of hot less dense particles which loses its heat with distance as shown by change in colour. In between the two isotherm walls, there is mixing of air particles which is a relatively warm region. In 16 c and d temperature uniformity is achieved. In conclusion it is evident that maximum temperature decreases with increase in Rayleigh number.

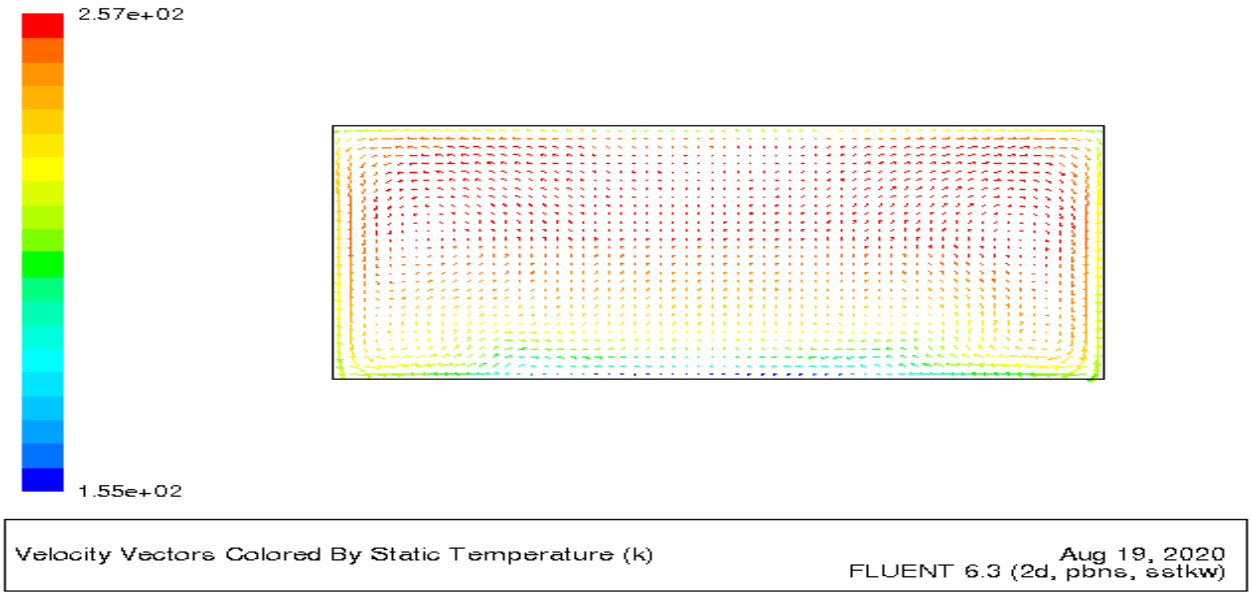

Fig 6.1.1 Isotherms of Rayleigh number $\mathbf{10^{10}}$**.**

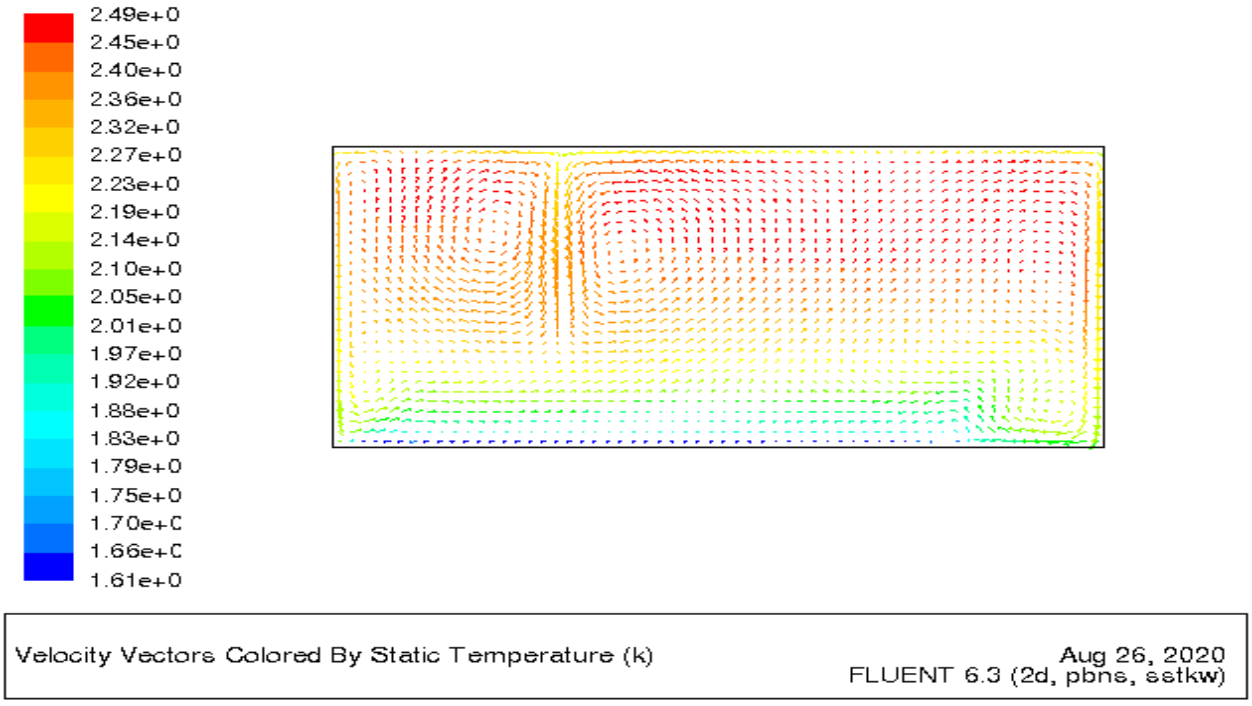

Fig 6.1.2 Isotherms of Rayleigh number $\mathbf{10^{11}}$**.**

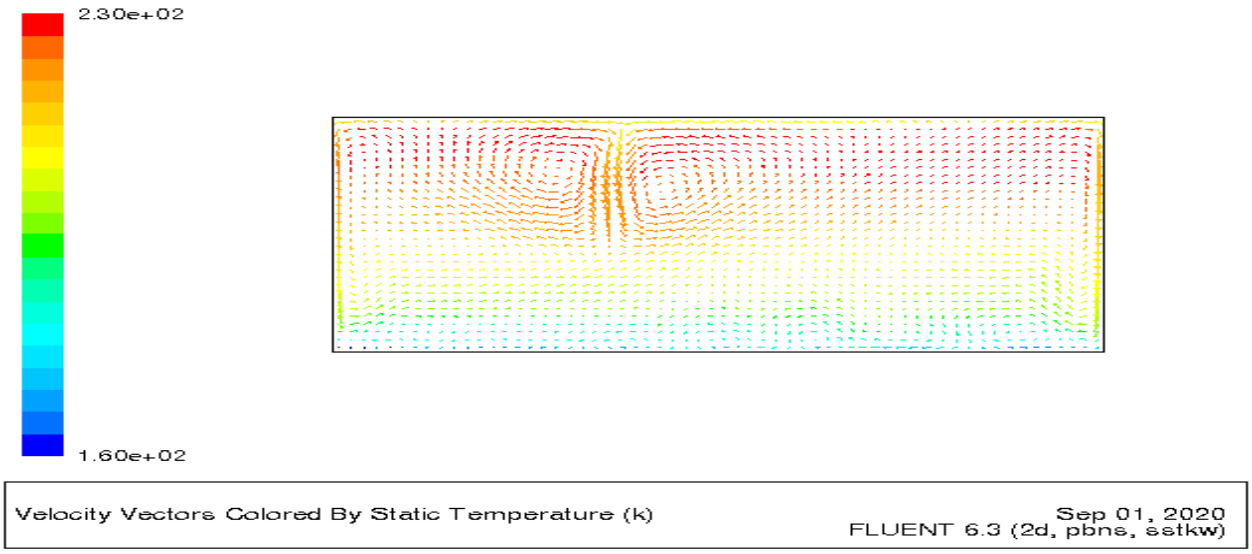

Fig 6.1.3 Isotherms of Rayleigh number $\mathbf{10^{12}}$**.**

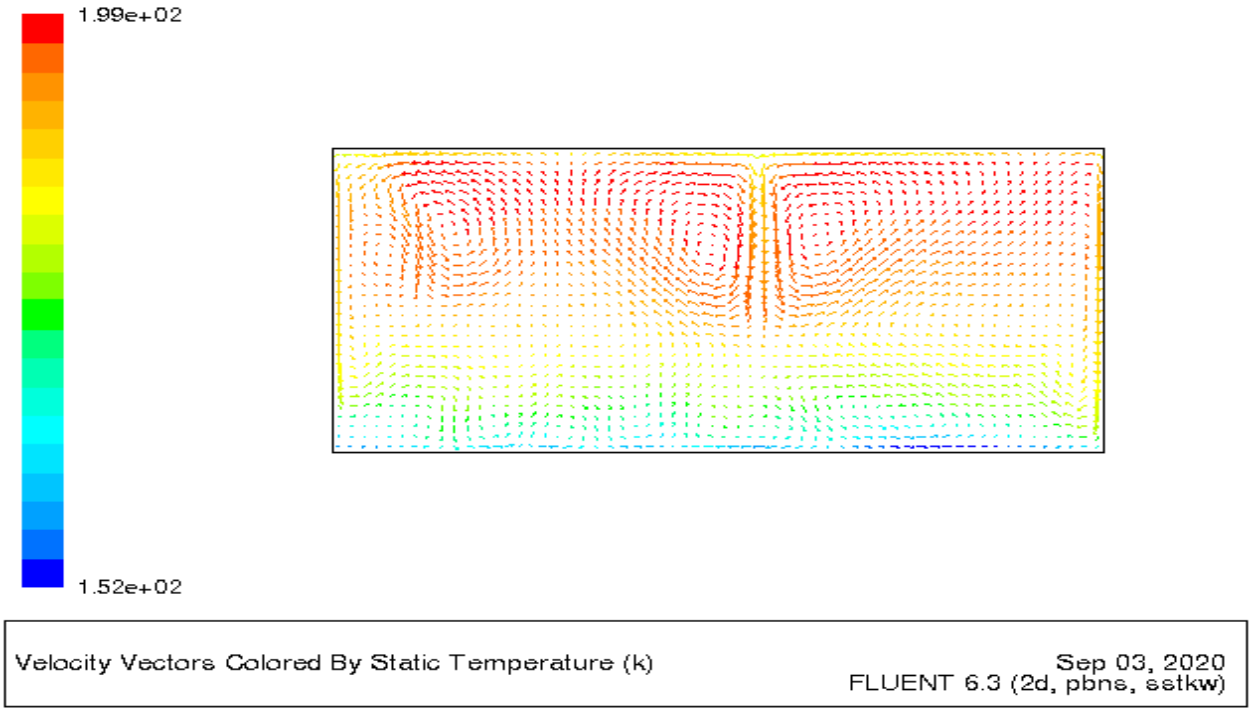

Fig 6.1.4 Isotherms of Rayleigh number $\mathbf{10^{13}}$**.**

6.2 Contours of velocity magnitude

In 6.2.1, the highest velocity of air particles is 0.522m/s, in 6.2.2, the highest velocity is 0.555m/s, in 6.2.3, the highest velocity is 0.593m/s and in 6.2.4, the highest velocity is 0.870m/s. In 6.2.1 the highest speed is at the middle at the mixing region. Vortices are more in 6.2.1 which become parallel as the Rayleigh number increases in 6.2.4 the vortices are parallel than any other set-up in this study and at this point is evident that as the Rayleigh number increases the flow becomes less turbulent.

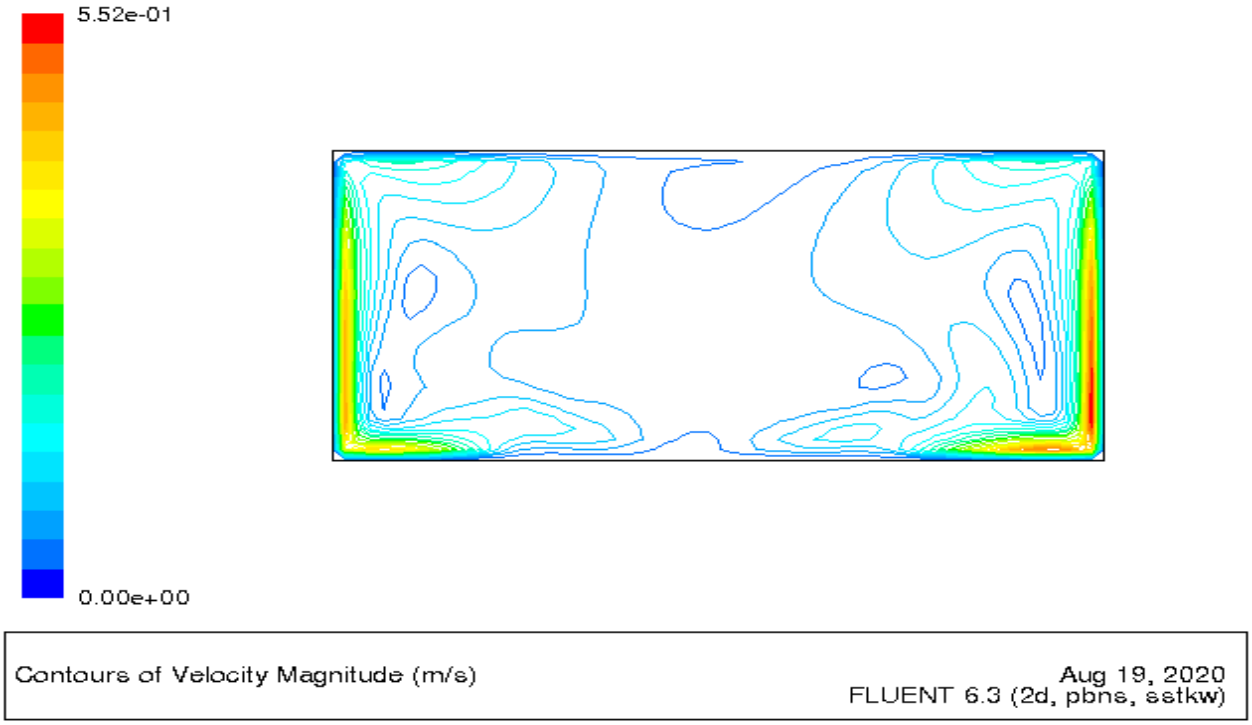

Fig 6.2.1 contours of velocity magnitude of Rayleigh number $\mathbf{10^{10}}$**.**

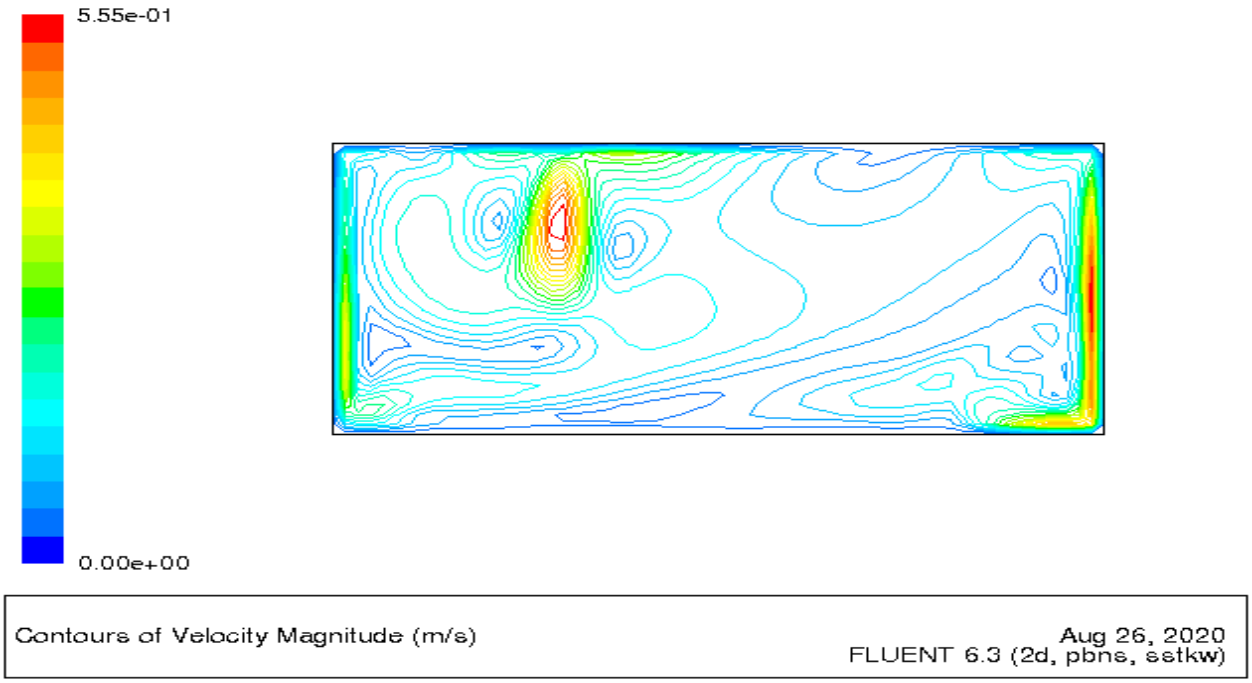

Fig 6.2.2 contours of velocity magnitude of Rayleigh number $\mathbf{10^{11}}$**.**

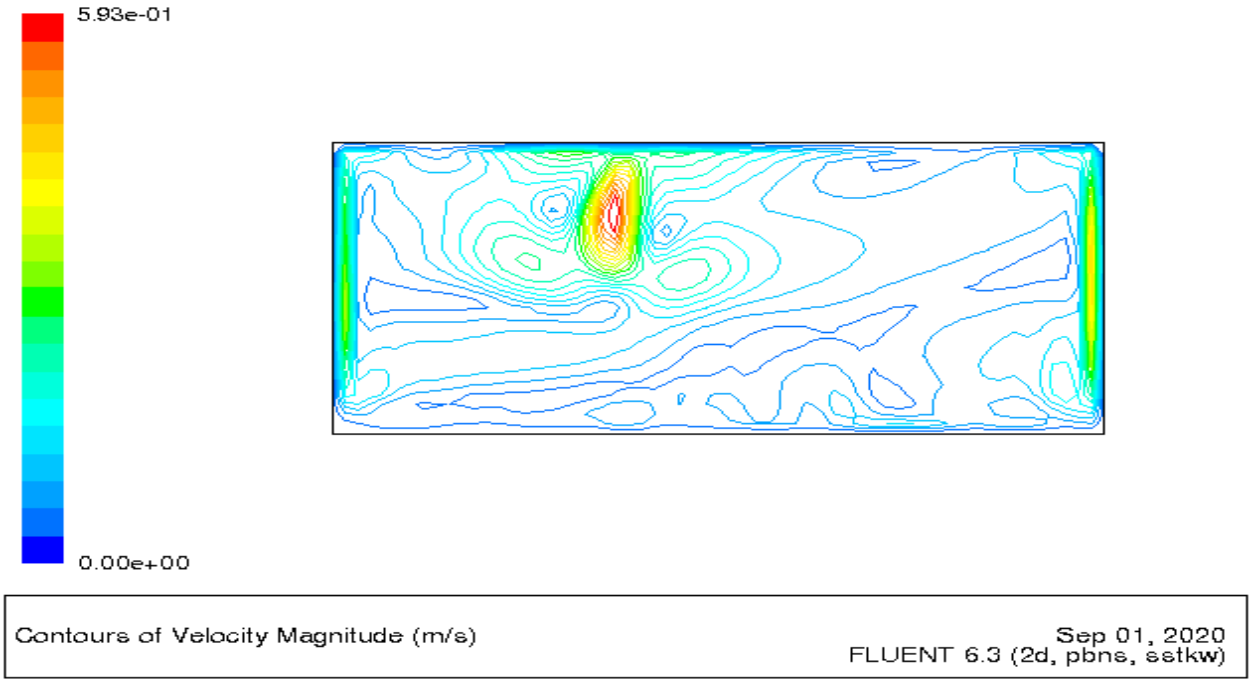

Fig 6.2.3 contours of velocity magnitude of Rayleigh number $\mathbf{10^{12}}$**.**

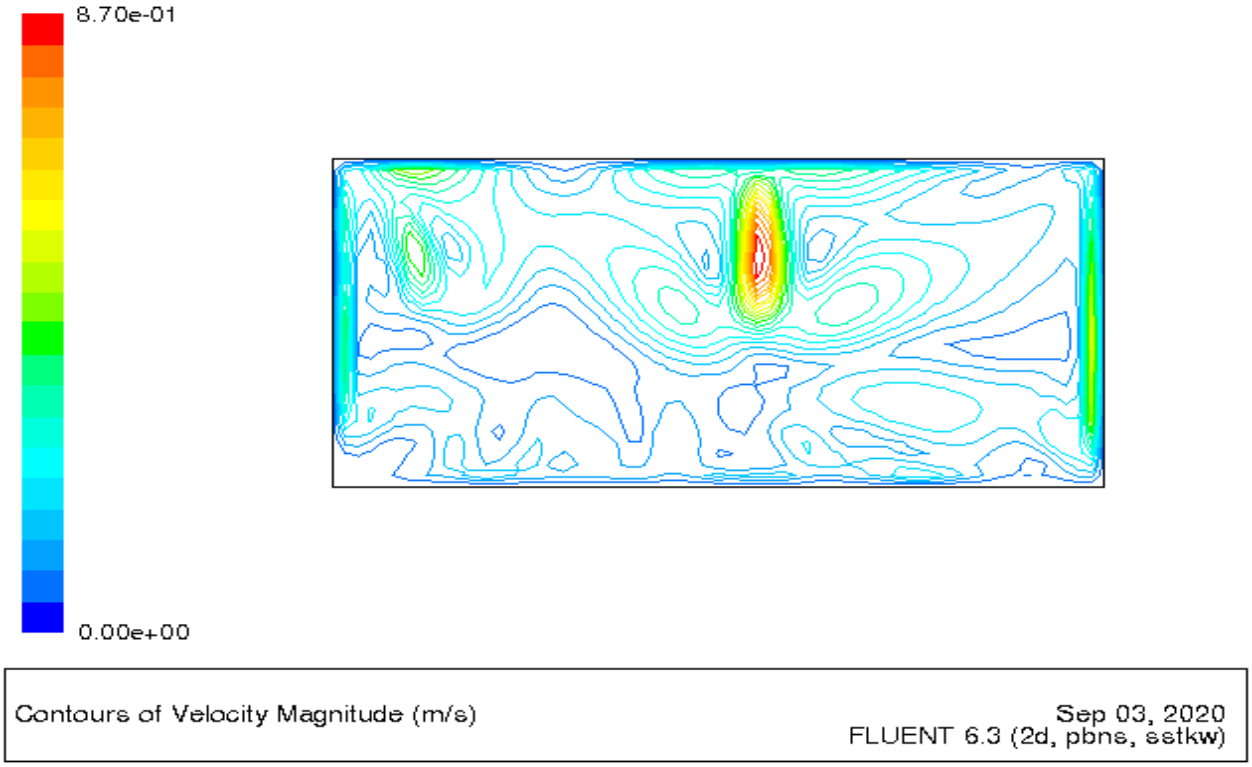

***Fig 6.2.4 contours of velocity magnitude of Rayleigh number* 10^{13}.**

6.3 Streamline distribution

Streamline is an imaginary line in a fluid such that the tangent at any point shows the path of the speed of an element of the fluid at that point. The lowest value indicated is of the Rayleigh number 10^{10} which is 0.100kg/s followed by that of Rayleigh number 10^{11} which is 0.233kg/s. This value increases as the Rayleigh number increases as depicted by that of a Rayleigh number 10^{12} which is 0.406kg/s and the highest which is 1.310kg/s as shown by that of Rayleigh number 10^{13}. In the figure 6.3.1, the vortices are big in size and they assume a circular part which deforms as distance increases from their centres. In 6.3.2, the radius of centre circle reduces which as well decreases as the Rayleigh number increases to 10^{13} as seen in figure 6.3.3.

In 6.3.4, the two center cell deforms and takes an oval shape. The vortices become parallel as the Rayleigh number increases.

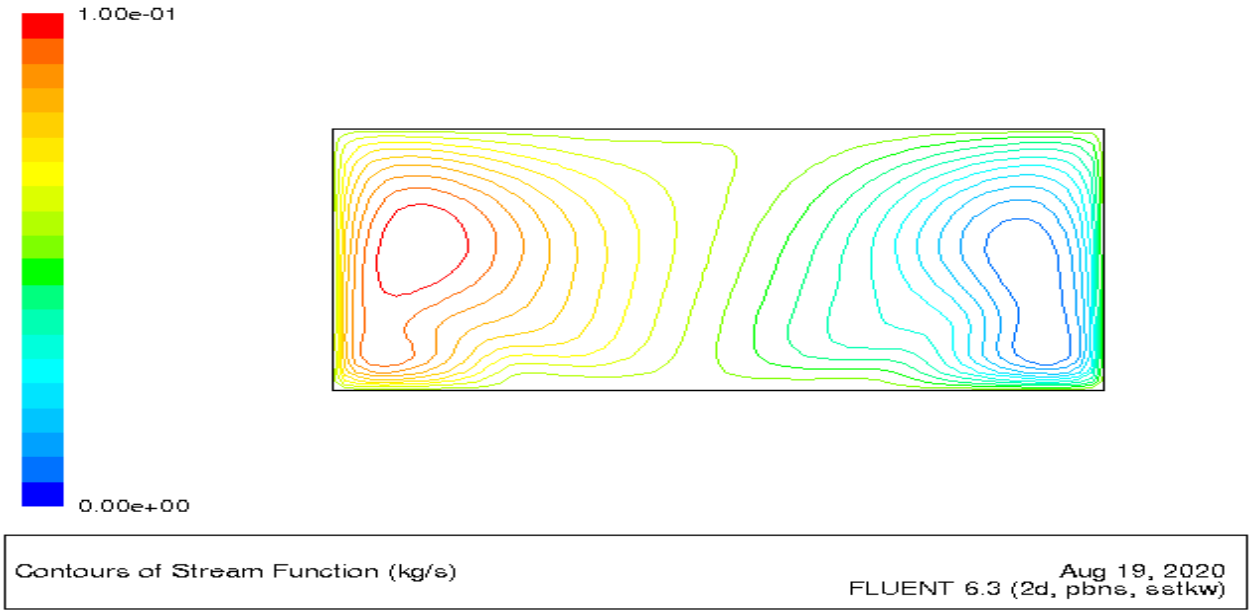

***Figure 6.3.1 contours of streamline of Rayleigh number* 10^{10}**

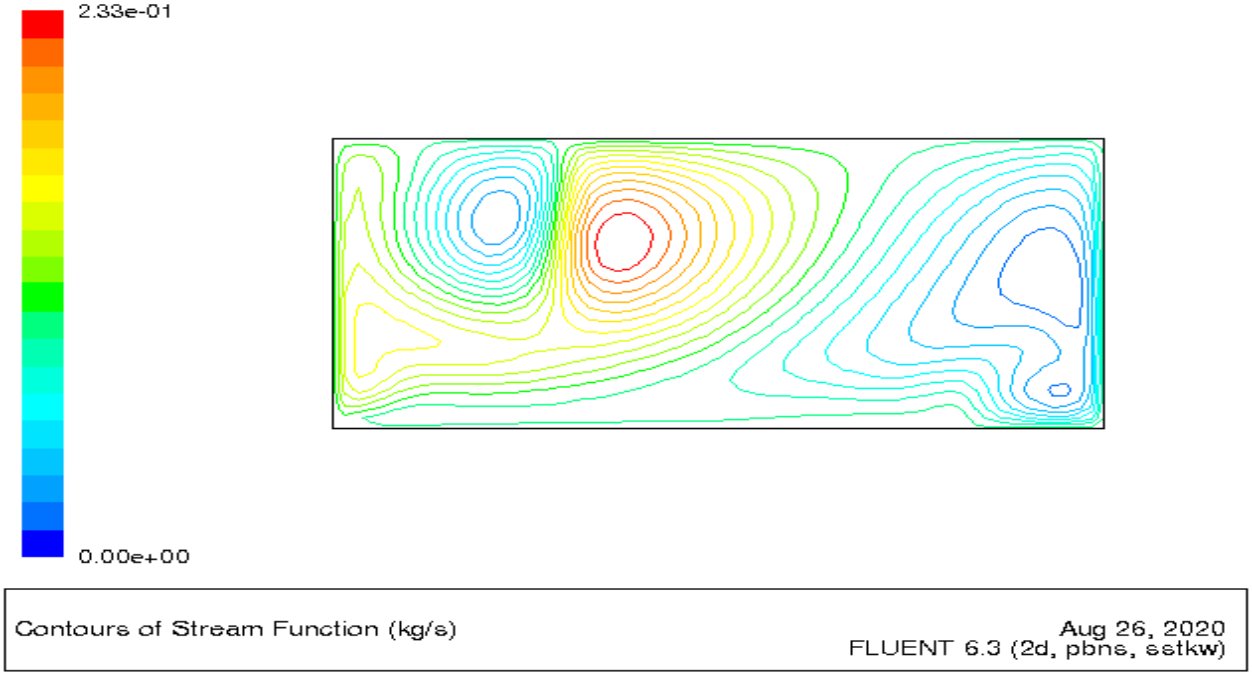

Figure 6.3.2 contours of streamline of Rayleigh number 10^{11}

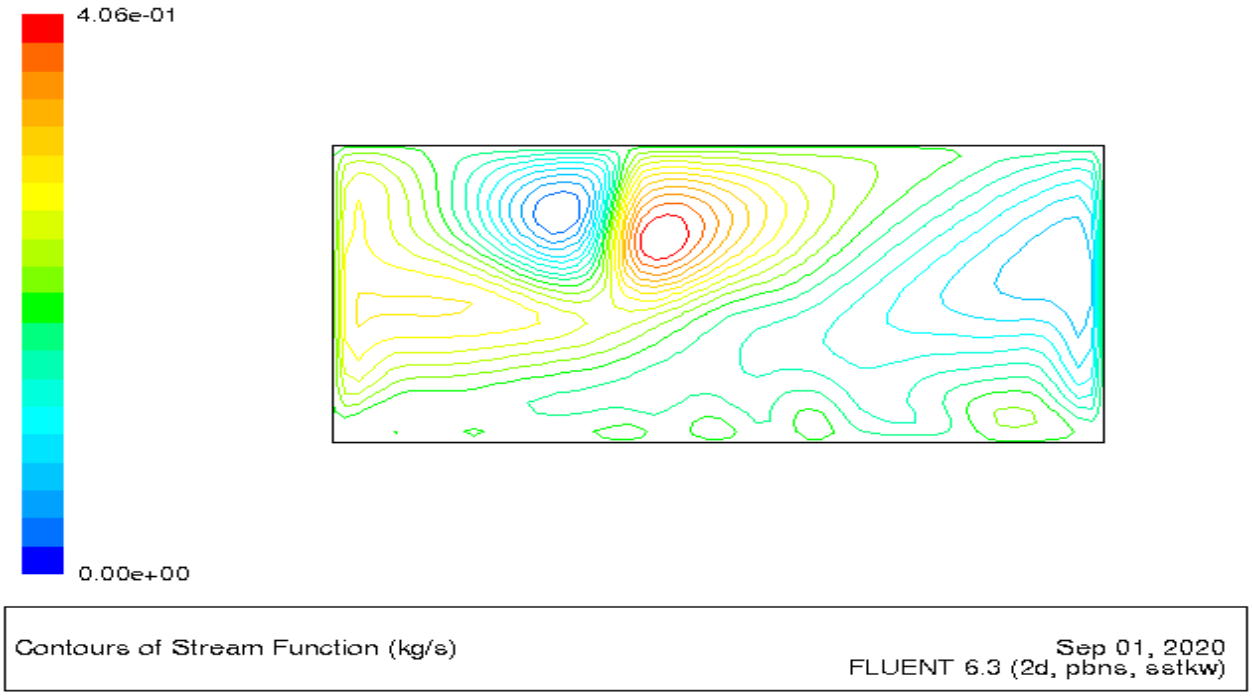

Figure 6.3.3 contours of streamline of Rayleigh number $\mathbf{10^{12}}$

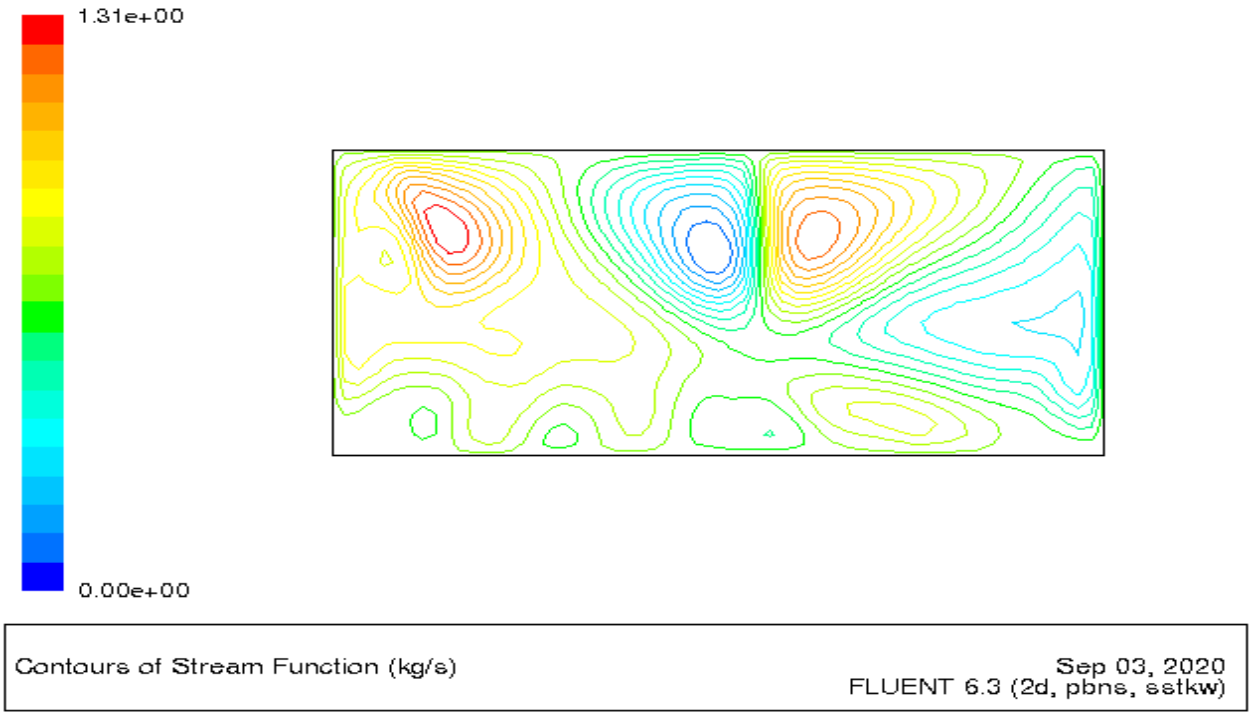

Figure 6.3.4 contours of streamline of Rayleigh number $\mathbf{10^{13}}$

6.4 Conclusion

The objective of the study was to simulate turbulent natural convention in a rectangular enclosure with localized heating and cooling. To achieve this, we had set up specific objectives which were achieved as follows:

Numerical data were set for k-ω-SST turbulence model. The boussinesq estimation were utilized allowing the conservation equation to be simplified. Discretization of governing equations with limit conditions were done using three-point forward and central difference approximations. Streamlines, Isotherms and Velocity magnitudes for Rayleigh numbers $10^{10}, 10^{11}, 10^{12} and\ 10^{13}$ were generated and showed that the increase in Rayleigh number decreased the turbulence.

The results showed that increased Rayleigh number decreased speed and vortices became more parallel thus decreasing turbulence. So the Rayleigh number has an important influence in temperature field and fluid stream in horizontal enclosure heated from the bottom of one of the sides.

It is also evident from the results obtained above that the position of the heater and the cooler greatly affected the distribution of heat in the enclosure. The heat distribution was found to be better when the heater and cooler were placed on the same side of the wall and it also increased with increase in Rayleigh number.

6.5 Recommendations

Further investigations are recommended for:

i. Enclosures with a three dimensional configurations.
ii. Varying the characteristics of the fluid contained in the enclosure.
iii. Effect of varying the operating temperature.

REFERENCES

Awuor K. (2012), Turbulent Natural Convection in an enclosure ; Numerical Study of Different k-epsilon models, Ph.D. Thesis, Kenyatta University, Kenya, 1-102.

Currie, I.G (1974). Fundamental of Fluids, McGraw-Hill Inc.

Edward, M., Sigey, J., OKello, J., &Okwoyo, J. (2013). Natural Convection with Localized Heating and Cooling on opposite Vertical Walls in an Enclosure. *CNCE,* 1(4), 72-78.

Goodarzi, M., m Safaei, M. R., Karimipour, A., Hooman, K., Dahari, M., Kazi, S. N., &Sadeginezhad, E. (2014). Comparison of the finite volume and lattice Boltzmann methods for solving natural convection heat transfer problems inside cavities and enclosures. In Abstract *and Applied Analysis (*Vol.2014). Hindawi.

Josephs K., Grace W.G., Francis K.G (2018).A Numerical investigation of Turbulent

Convectionin 3-D Enclosure using k-ω-SST Model and SIMPLEC Method.

International Journal of Engineering Science and Research Technology.

Khanal, R., & Lei, C. (2015). A numerical investigation of buoyancy induced turbulent air flow in an inclined passive wall solar chimney for natural ventilation . *Energy and Buildings, 93, 217-226.*

Kimunguyi, K. J. (2016). *A numerical investigation of turbulent natural convection in a 3-d enclosure using k-ω- SST model and piso method (*Doctoral dissertation, Kenyatta University).

Safaei, M., Goodarzi, M., & Mohammad, M. (2016). Numerical modelling of turbulence mixed convection heat transfer in air filled enclosures by finite volume method. *The International Journal of Multiphysics 5(4).*

Sajjadi, H., &Kefayati, R. (2015). Lattice Boltzmann simulation of turbulent natural convection in tall enclosures. *Thermal Science, 19(1), 155*-166.

Wu, T., & Lei, C. (2015). On numerical modelling of conjugate turbulent natural convection and radiation in a differently heated cavity. *International Journal of Heat and Mass Transfer, 91, 454-466.*

Zimmermann, C., &Groll, R. (2014). Modelling turbulent heat transfer in natural convection flow. *Journal of Applied Mathematics and Physics,* 2(07), 662.

Boussinesq, M., & Porporato, A. (1877). *A Class of Exact Solutions of the Boussinesq Equation for Horizontal and Sloping Aquifers.*

Reynolds, M. (1895). *Direct numerical simulation of a differentially heated cavity of aspect ratio 4 with Rayleigh numbers up to 10(11) - Part I: Numerical methods and time-averaged flow*.

Rodi, E. (1993). *Numerical flow simulation II*. Berlin: Springer.

Incropera, G., & Dewitt. (2002). Numerical simulation of the flow and heat transfer around a cylinder with a pulsating approaching flow at a low Reynolds number. *Proceedings of the Institution of Mechanical Engineers, Part C: Journal of Mechanical Engineering Science*, *215*(1), 105-119.